Application of combustion and DTA-TGA analysis to the study of metamorphic organic matter

SCHWEIZ. MINERAL. PETROGR. MITT. 82, 33–53, 2002

Application of combustion and DTA-TGA analysis to the study of metamorphic organic matter

by *Tatiana V. Petrova*[1*], *Rafael Ferreiro Mählmann*[1], *Willem B. Stern*[1] and *Martin Frey*[1†]

Abstract

Coalification of organic matter in the North Penninic Bündnerschiefer of eastern Switzerland has been studied using combustion analysis, thermal analysis and X-ray diffraction. Organic matter used for analysis was characterized by optical microscopy (maceral analysis). Combustion analysis was applied with most encouraging results to determine metamorphic grade. Results correlate well with the known metamorphic pattern and also additional information relevant to the tectono-metamorphic history. Two types of CO_2 peaks are recognized: a sharp narrow (type-S) peak and a broad (type-B) peak. Distribution of these peak types is regular in samples taken along the metamorphic profile, from high diagenesis to lower amphibolite facies conditions. The combustion temperatures of organic matter increases essentially with increasing metamorphic grade, while the total weight loss decreases slightly. Combustion analysis and differential thermal - thermal gravimetric analysis have proven to be useful in characterizing metamorphic organic matter and in detecting heterogeneities therein.

Keywords: Combustion analysis, organic matter, graphitization, North Penninic Bündnerschiefer, Central Alps.

1. Introduction

Carbonaceous material (CM) is a common constituent of metamorphic rocks. In metasedimentary rocks organic matter (OM) is the predominant form of CM. With increasing coalification, amorphous organic products are converted into ordered anisotropic structures and finally, during graphitization, transformed to a crystalline and pure carbon-material, with graphite as the end product (TEICHMÜLLER, 1987). Conversion of OM to graphite includes the loss of hydrogen, nitrogen, and oxygen, while polymerization proceeds to form larger, more complex, carbon-rich units (BUSECK and BO-JUN, 1985).

In general, graphitization proceeds in several steps: 1) development of planar networks of hexagonal carbon rings; 2) stacking of the planar carbon networks to form a layered structure of two-dimensional symmetry; 3) formation of a three-dimensional structure (DEMENY, 1989). These micro-structural transformation steps are optically visible and subdivided into: (1) organic matter; (2) transitional matter (partly coke-like); (3) optical graphite (DIESSEL et al., 1978). "Optical graphite" found in the stage of the semi-graphite coal rank (DIN-classification) does not correspond to true graphite in the sense of a mineral, as it is still highly disordered at low metamorphic grade.

The degree of OM crystallization is related to the grade of metamorphism (BUSECK and BO-JUN, 1985) and the intensity of strain ("shear stress", TEICHMÜLLER and TEICHMÜLLER, 1954; TEICHMÜLLER, 1987). In contrast to many mineral transformations during metamorphism, graphitization of CM (e.g. OM) is strictly an irreversible process (PESQUERA and VELASCO, 1988). Structural, chemical and thermal studies of OM may provide useful informations on the metamorphic history and the determination of metamorphic grade in metasedimentary rocks from diagenetic conditions to very low and medium grade.

Numerous studies have investigated the graphitization process of CM/OM by optical microscopy (e.g. RAGOT, 1977; DIESSEL et al., 1978; TEICHMÜLLER, 1987), by X-ray diffraction (LANDIS,

[1] Institute of Mineralogy and Petrography, Bernoullistrasse 30, CH-4056 Basel, Switzerland. <Rafael.Ferreiro-Maehlmann@unibas.ch>
[*] Present address: T. Hürlimann Petrova, Fröschenweg 13, 4127 Birsfelden.
[†] Martin Frey died in an accident in the Swiss Alps on September 10, 2000.

1971; GREW, 1974; ITAYA, 1981; OKUYAMA-KUSUNOSE and ITAYA, 1987), Raman spectroscopy (PASTERIS and WOPENKA, 1991; WOPENKA and PASTERIS, 1993; YUI et al., 1996; SPÖTL et al., 1998) and stable isotopes (HOEFS and FREY, 1976; MORIKIYO, 1984; WADA et al., 1994). A very early differential thermal analysis (DTA) and X-ray diffraction study on "graphite", the first one in the Alps, was published by JÄGER and STRECKEISEN (1958). However, not many attempts (WADA et al., 1994; KAHR et al., 1996) have been made to correlate the stage of coalification defined by optical microscopy and the degree of graphitization with results of thermal analysis. The first systematic study along a metamorphic profile will be presented. This paper deals with the application of combustion analysis and differential thermal-thermal gravimetrical analysis (DTA-TGA) to study the metamorphism of carbonaceous organic material.

2. Geology, lithology, and mineralogy

The North Penninic Bündnerschiefer are marine to terrigenous sediments mostly comprising shaly to marly formations, with calcareous intercalations of sandstones and breccias (partly turbidites). In the youngest formations sandstones and siltstones are predominant (NÄNNY, 1948). Basaltic intercalations of MORB composition (TRÜMPY, 1980) within the Jurassic Bündnerschiefer metasediments (NÄNNY, 1948) probably represent local remnants of the North Penninic oceanic crust. The main mass of the Bündnerschiefer is of Cretaceous age (STEINMANN, 1994). During sedimentation of the Bündnerschiefer and North Penninic flysch formations of Tertiary age, the bathymetry changed from a oceanic deep sea to shallower facies, and from neritic to litoral conditions (NÄNNY, 1948; ZIEGLER, 1956; DIETRICH, 1976).

Based on regional geological studies, the North Penninic Bündnerschiefer are subdivided into the following structural units: Prättigau Bündnerschiefer, Prättigau Flysch, Grava nappe Bündnerschiefer, Tomül nappe Bündnerschiefer, Misox zone Bündnerschiefer (Fig. 1a). Careful stratigraphic and geochemical observations allowed STEINMANN (1994) to conclude that the Tomül nappe was originally a direct southern continuation of the Grava nappe. The Prättigau Bündnerschiefer seems to be the northern continuation of the Grava nappe, not limited against the latter by a thrust fault (WEH, 1998). The Misox zone Bündnerschiefer is the southern continuation of the Tomül nappe.

The metamorphic profile studied (Fig. 1) extends from the east of Landquart, from the northeastern corner of the Prättigau half window, to Mesocco. Samples collected include shales to phyllites, marls to carbonate phyllites, and dolomitic carbonates to marbles. The mineral contents of all lithologies is fairly uniform, with the main mineral assemblage (MA) being muscovite/phengite + chlorite + quartz + calcite + paragonite ± dolomite ± albite and ± detrital plagioclase. From south of Chur to Mesocco, plagioclase is partly replaced by white mica and clinozoisite. In a few samples biotite, chloritoid and Mg-carpholite were found by optical microscopy and microprobe studies. Garnet is present in a few samples of low to medium grade metamorphic conditions (around San Bernandino–Mesocco). Accessory minerals include pyrite (or pyrrhotite at higher metamorphic grade), rutile, zircon, and tourmaline. In total, 55 samples were collected, and these are fairly evenly distributed along the profile (Fig. 1). At some localities, several samples were taken, in order to control the heterogeneity in lithology and carbonaceous material (Fig. 1 and Table 1).

Metamorphic grade generally increases along the profile from NE to SW (WEH et al., 1996). In the Prättigau half window, Early Cretaceous Prättigau Bündnerschiefer reached lower greenschist facies; they are surrounded by anchizonal Late Cretaceous Bündnerschiefer and Prättigau Flysch to the north, east and south. At the lowest metamorphic grade, high diagenetic conditions were found to the northeast of Landquart (samples 1 and 2, Fig. 1b; see also THUM and NABHOLZ, 1972; FERREIRO MÄHLMANN, 1994). Metamorphic grade decreases continuously from the Bündnerschiefer towards the overlying Prättigau Flysch (WEH et al., 1996).

Bündnerschiefer of the Grava and Tomül nappes reached greenschist to blueschist facies metamorphism (FREY and FERREIRO MÄHLMANN, 1999). Evidence for a low temperature - high pressure metamorphic overprint include (Fe-Mg)-carpholite and chloritoid zone boundaries. As suggested by OBERHÄNSLI et al. (1995), these show an increase in metamorphic grade from Chur (270 to 350 °C, 7.5 kbar) towards the west (350 to 400 °C, 15 kbar). Blueschist assemblages were overprinted under greenschist facies conditions (WEH, 1998), as also indicated by an increase in vitrinite reflectance from the northeast (WEH et al., 1996) at Chur (300 ± 20 °C) to the southwest (400 ± 40 °C) or from north to south (FERREIRO MÄHLMANN and PETSCHICK, 1997).

The geology and metamorphism of the Misox zone Bündnerschiefer were investigated by mineralogical studies of metapelites and marbles by

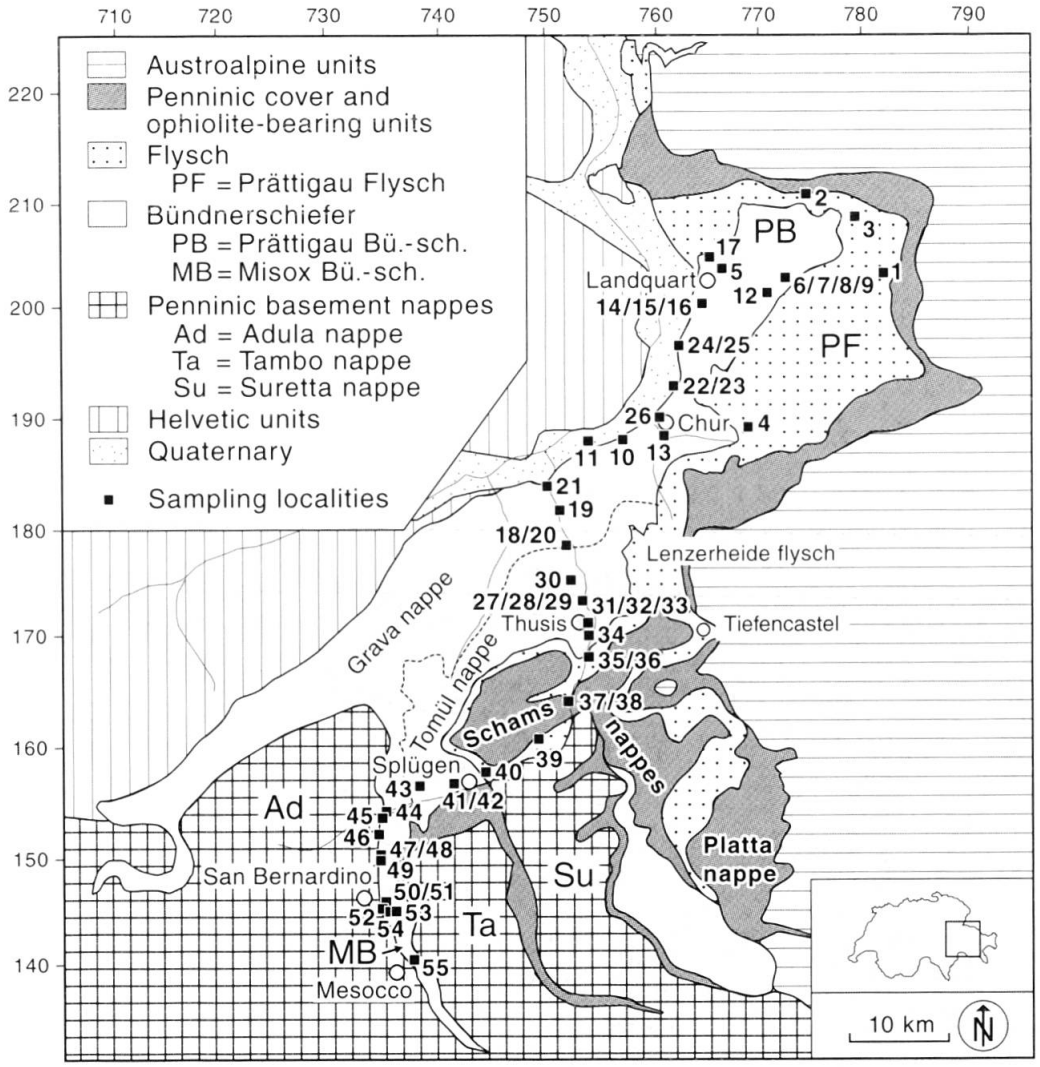

Fig. 1a Schematic tectonic map of the North Penninic Bündnerschiefer in eastern Switzerland. Numbers refer to sample list (Table 1). Middle Penninic nappes – Tambo, Suretta and Schams nappes, Bü – Bündnerschiefer.

TEUTSCH (1982) who found that amphibolite facies was reached. The "staurolite isograd" (500–550 °C, 6 kbar) was mapped at the level of Mesocco (THOMPSON, 1976).

In summary, the metamorphic grade in the profile studied increases generally from anchizone to greenschist to amphibolite facies (Fig. 1b), with relics of high pressure-low temperature metamorphism (blueschist facies) in the Bündnerschiefer of the Grava and Tomül nappes (OBERHÄNSLI et al. 1995; FREY et al., 1999; FREY and FERREIRO MÄHLMANN, 1999).

3. Analytical techniques

3.1. EXTRACTION OF CARBONACEOUS MATERIAL

For X-ray diffraction analysis the carbonaceous material must be separated from the other mineral components because the strongest quartz (101) reflection and the (006) reflection of mica coincide with the only strong graphite (002) reflection.

After disintegrating the rock material (1.0 to 2.0 kg) with a hammer and subsequent short grinding in a tungsten carbide mill, the carbonates were removed in a platinum crucible by concentrated hydrochloric acid (38%). In a next step, the mixture (20–30 mg) was periodically stirred and heated to 40–50 °C during 3–5 hours in order to accelerate the destruction of silicates such as clay minerals and mica by hydrochloric and nitric acids. Afterwards, the solution was then carefully filtered with distilled water and placed in concentrated hydrofluoric acid (48%) in order to remove quartz. To remove quartz and sheet silicates completely, acid treatment was repeated at least three times with each of these acids, and with careful washing and filtering following each step. Evenso, a residue of insoluble rutile, tourmaline, zircon, pyrite, garnet, and pyrrhotite remained.

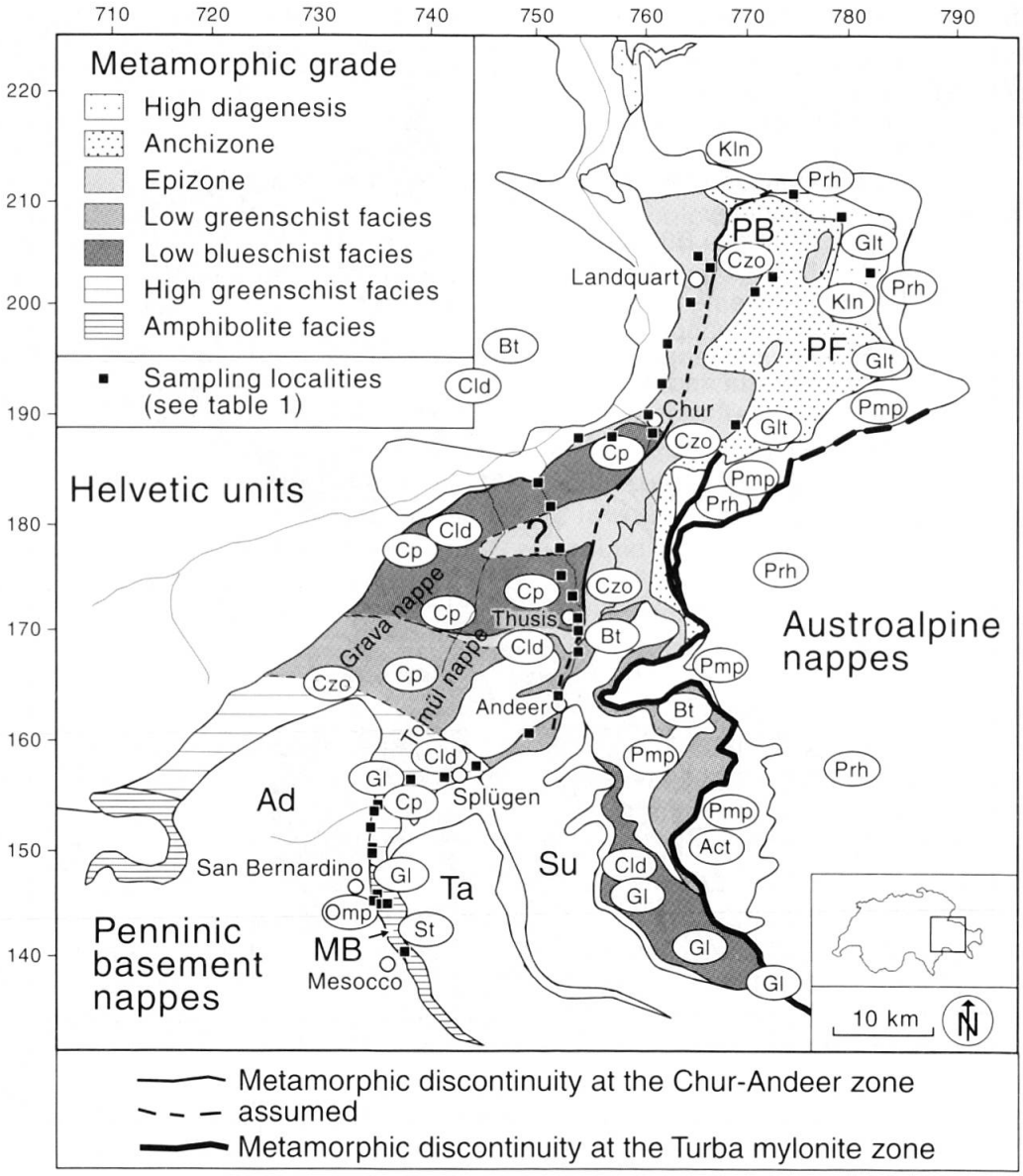

Fig. 1b The metamorphic sketch map is based on the "The new metamorphic map of the Alps" (FREY et al., 1999; FREY and FERREIRO MÄHLMANN, 1999), the metamorphic map from WEH et al. (1996), data from OBERHÄNSLI et al. (1995), data from FERREIRO MÄHLMANN (1996) and results from this study. On the map the index minerals occurrences of the Tertiary LT-LP to MT-LP metamorphism (Glt – glauconite, Kln – kaolinite, Prh – prehnite, Pmp – pumpellyite, Act – actinolite, Czo – clinozoisite, Bt – biotite, Cld – chloritoid, St – staurolite) and the older LT-HP metamorphism (Cp – carpholite, Gl – glaucophane and Omp – omphacite) are shown.

GREW (1974) reported the formation of unidentifiable fluorides that had to be removed by heating samples for 1 to 6 hours in a large excess of acid aluminum chloride solution. As observed by CASTRO REIS and CANTO MACHADO (1992), samples rich in chlorite or/and feldspar, both of which are abundant in some of the Bündnerschiefer samples, resulted in the formation of complex fluorides after acid treatment. Although these complexes do not interfere with the carbon diffraction pattern, they effectively dilute the sample and thus lower carbon detection limits. For samples rich in chlorite the diffraction pattern of a fluorosilicate by-product was similar to that of $KMgAlF_6$. For samples rich in feldspar and quartz a fluorosilicate that had formed during acid treatment was identified as K_2SiF_6 by X-ray diffraction (CASTRO REIS and CANTO MACHADO, 1992).

In this study, the formation of synthetic fluorite and fluorides ($KMgAlF_6$) was observed only at the first stages of hydrofluoric acid treatment. The problem was avoided by first dissolving carbonate in the whole rock sample and subsequently treating it with strong hydrochloric and nitric acid (as described above), and by careful filtering prior to subsequent treatment with hydrofluoric acid.

3.2. X-RAY DIFFRACTION

Measurements were performed on a Siemens/Bruker-AXS D-5000 diffractometer. Excitation conditions were Cu 40 kV, 30 mA, a graphite secondary monochromator, automatic divergence and antiscatter slits, but no primary filter were used. Since only very little material remained after acid treatment, a micro-preparation method (HANDSCHIN and STERN, 1989) was used, with 1 to 5 mg of OM concentrate fixed on a stretched polypropylene foil with a surface area of >12 cm^2. Although slow-motion runs were performed, counting statistics were often insufficient due to dilution of OM by zircon, rutile etc. being present as main components in the concentrates (Fig. 2).

3.3. COMBUSTION ANALYSIS

Combustion analysis on OM concentrates was performed in the temperature range of 60 to 1100 °C, using a RC-412 multiphase carbon determinator. The carrier gas was oxygen, with a gas flow of 50 ml/min. A heating rate of 70 °C/min was used, i.e. combustion analysis was performed in a *dynamic* rather than in a *static* mode. This allowed us to register the combustion peak temperatures but not the mass proportions of individual reaction processes, at the expense of much longer analysis times than in static mode.

Combustion analysis in the temperature range used here registers signals of carbon, carbondioxide and water released during the heating of a sample between 60 and 1100 °C by means of infrared cells. Other compounds are not determined with the equipment used, a disadvantage in the analysis of carbonaceous material containing nitrogen and sulfur as well. Nevertheless, application of combustion analysis in metamorphic studies of CM is useful because it determines (a) carbon dioxide and water contents in CM, both of which change with metamorphic grade, and (b) the exact temperatures at which carbon dioxide or water are released. These temperatures are expected to rise with increasing degree of graphitization due to increasing thermal resistance of OM.

Since several reactions may occur in the same temperature range, peak overlap may jeopardize quantification of the peak temperatures and peak areas as a measure of the mass fractions involved. To solve this problem, combustion data were first processed in a spreadsheet to linearize temperature, then fitted/deconvoluted using a fitting pro-

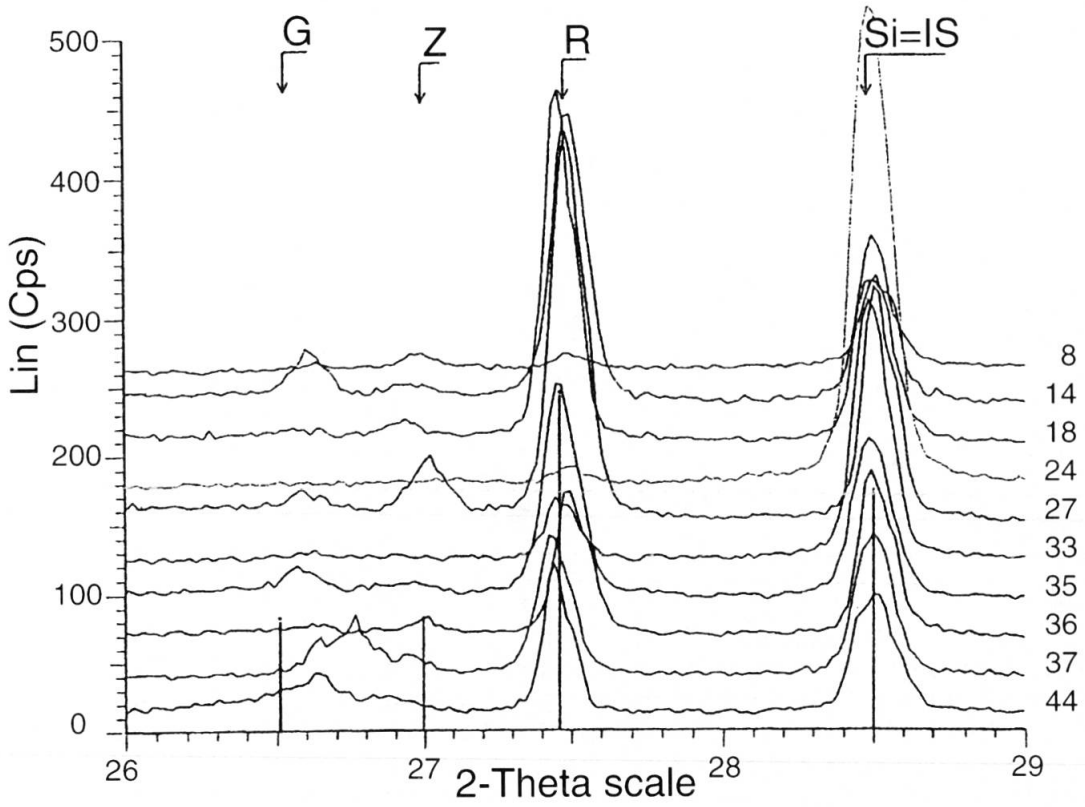

Fig. 2 Combined X-ray diffractograms of ten different representative carbonaceous material concentrates. Metamorphic grade increases downwards, numbers refer to the sample list of Table 1. The most prominent reflection is from rutile, but does not interfer with graphite. Reflections: G – graphite (002), R – rutile (110), Z – zircon (200), IS – Internal standard Si (111), silicon powder added.

gram originally designed for crystallographic work. Since reaction peaks need not be symmetrical or Gaussian, a Split-Pearson option was used to determine peak temperatures and estimate peak areas (Fig. 3). A Pearson VII function best applies for well and badly crystallized (ordered) carbonaceous material and for small and strong peaks.

3.4. THERMAL ANALYSIS

The instrument used (SDT 2960 from TA Instruments, Inc. USA) simultaneously performs both thermo-gravimetric and differential thermal analysis (TGA and DTA). The carrier gas was oxygen, with a gas flow of 100 ml/min. The heating rate was usually 20 °C/min, and the temperature range

Table 1 Sample list and results of illite crystallinity ($\Delta° 2\Theta$), maximum vitrinite reflectance measurements (R_{max}%), thermal and combustion analyses of organic matter concentrates. OG – optical graphite. Row 7 and 9 show illite crystallinity (IC) and vitrinite reflectance (VR) variations from samples close (in an area around 500 m²) to the sample locality indicated in row 1. HW – half width, Resid – insoluble residue.

Location of the samples						IC	VR	VR	Thermal Analysis		
No.	Sample origin	Tectonic unit	Height [m]	Swiss Grid x-coord.	Swiss Grid y-coord.	illite crystallinity variation from 2 to 10 samples	Vitrinite reflection mean [Rmax%]	reflectance variation from 2 to 4 samples [Rmax%]	maximum reaction temperature	weight loss	peak area
1	ES2/RFM	F	2170	203.265	782.160	0.45 – 0.42	**3.0**	3.0	425	53.5	31.6
2	MF2986	F	2150	211.700	775.300	0.42 – 0.38	**3.6**	3.6	441	41.1	15.5
3	MF2987	F	1830	208.700	779.400	0.40 – 0.36	**4.8**	5.0 to 4.4	482	42.7	67.0
4	PS7/RFM	F	1200	189.195	768.940	0.34 – 0.32	**5.6**	5.6 to 5.0	588	35.0	65.8
6	MW9664	F	680	203.010	772.485	0.28 – 0.22	**5.7**	5.8 to 5.6	550	86.7	48.6
7	TP01	P	690	202.825	772.575	0.28 – 0.22	**5.7**	5.8 to 5.6	–	–	–
8	TP02	P	690	202.825	772.575	0.28 – 0.22	**5.7**	5.8 to 5.6	455	64.5	32.4
9	TP03	P	690	202.825	772.575	0.28 – 0.22	**5.7**	5.8 to 5.6	480	72.7	28.0
10	TP09	G	1030	188.100	756.850	0.20 – 0.18	**5.7**	7.0 to 5.7	561	13.4	39.2
12	SS2/RFM	P	1280	189.195	768.940	0.26 – 0.20	**6.0**	6.0 to 5.5	487	35.2	52.9
14	TP04	P	1060	200.300	764.375	0.22 – 0.20	**6.8**	6.9 to 6.0	489	55.5	66.6
15	TP05	P	1060	200.300	764.375	0.22 – 0.20	**6.8**	6.9 to 6.0	–	–	–
16	TP06	P	960	200.300	764.375	0.22 – 0.20	**6.8**	6.9 to 6.0	494	69.9	37.8
18	TP41	G	670	177.300	751.850	0.20 – 0.18	**7.0**	7.4 to 6.0	585	48.2	–
19	TP12	G	630	181.750	751.275	0.20 – 0.16	**7.1**	7.2 to 5.8	569	45.3	29.6
21	TP11	G	680	183.900	750.150	0.20 – 0.18	**7.5**	7.5 to 7.0	516	48.5	29.2
22	TP43	P	800	192.900	761.600	0.20 – 0.18	**7.5**	7.5	479	55.5	44.8
23	TP44	P	800	192.900	761.600	0.20 – 0.18	**7.5**	7.5	463	46.4	–
24	TP07	P	970	196.500	762.125	0.21 – 0.17	**7.7**	7.9 to 7.0	477	45.9	36.0
25	TP08	P	970	196.500	762.125	0.21 – 0.17	**7.7**	7.9 to 7.0	491	34.1	34.0
27	TP13	T	700	173.325	753.300	0.19 – 0.16	**8.0**	8.4 to 7.5	600	42.4	43.3
28	TP14	T	700	173.325	753.300	0.19 – 0.16	**8.2**	8.4 to 7.5	559	25.7	56.2
29	TP15	T	700	173.325	753.300	0.19 – 0.16	**8.2**	8.4 to 7.5	602	27.5	47.6
30	TP39	T	760	175.350	752.350	0.18 – 0.14	**8.5**	8.5 to 7.0	–	–	–
31	TP16	T	860	171.125	753.775	0.18 – 0.15	**9.4**	10.0 to 7.5	564	40.4	47.5
32	TP17	T	860	171.125	753.775	0.18 – 0.15	**9.4**	10.0 to 7.5	588	38.0	53.5
33	TP18	T	860	171.125	753.775	0.18 – 0.15	**9.4**	10.0 to 7.5	554	47.4	49.3
35	TP20	T	900	168.025	753.775	0.18 – 0.13	**OG**	14.0 to 10.0	506	34.1	64.4
36	TP21	T	900	168.025	753.775	0.18 – 0.13	**OG**	–	582	36.2	41.2
37	TP37	F	1000	164.050	752.000	0.18 – 0.13	**OG**	–	459	27.2	–
41	TP22	M	1620	156.675	741.225	0.14 – 0.12	**OG**	–	596	38.8	57.1
42	TP23	M	1650	156.675	741.225	–	**OG**	–	582	45.1	57.0
43	TP24	M	1770	156.475	738.125	0.14 – 0.12	**OG**	–	588	44.5	46.3
44	TP25	M	1800	154.200	735.325	–	**OG**	–	613	29.6	47.2
50	TP26	M	1640	145.925	735.325	–	**OG**	–	606	22.2	29.3
51	TP27	M	1640	145.925	735.325	–	**OG**	–	597	38.6	58.1
52	MF1885	M	1850	144.350	735.875	–	**OG**	–	618	6.2	56.8
54	TP28	M	1610	144.950	735.550	–	**OG**	–	610	26.6	54.7
55	MF2042	M	900	140.450	737.600	–	**OG**	–	634	9.0	41.8

Samp.	Combustion Analysis [O_2] and [H_2O]						Combustion Analysis [O_2]					Combustion Analysis [O_2]					Combustion Analysis [O_2]				
	CO_2	H_2O			CO_2 peak	H_2O peak	CO_2 S-type peaks					CO_2 B-type peaks					H_2O				
No.	tot [%]	tot [%]	Sum [%]	Resid [%]	tot Area	tot Area	T°C	Area	HW	abs [%]	rel [%]	T°C	Area	HW	abs [%]	rel [%]	T°C	Area	HW	abs [%]	rel [%]
1	16.0	26.2	42.2	46.5	14458	2090	363	4328	0.4	4.8	30	503	2364	6.2	2.6	16	350	1991	15.0	25.0	95
2	24.4	1.5	25.9	59.0	17513	1125	410	2833	0.4	4.0	16	538	3186	4.7	4.5	18	440	1037	12.9	1.4	92
3	10.3	6.9	17.2	57.1	17062	1455	362	7042	0.5	4.3	41	512	6555	7.5	4.0	38	218	1177	5.5	5.6	81
4	44.7	7.5	52.2	65.0	1657	–	–	–	–	–	–	595	990	4.2	26.7	60	–	–	–	–	–
6	50.0	50.0	100.0	13.3	23960	3359	387	6544	0.4	13.7	27	539	3529	4.3	7.4	15	265	2957	8.2	44.0	88
7	5.2	10.7	15.9	52.1	8165	1387	356	5656	0.4	3.6	69	457	935	4.0	0.6	11	209	862	11.4	6.7	62
8	10.2	6.1	16.3	35.7	6596	–	382	1468	0.4	2.3	22	600	1788	6.4	2.8	27	–	–	–	–	–
9	33.3	3.4	36.7	27.3	24416	719	381	5020	0.4	6.8	21	608	10676	6.6	14.6	44	235	456	12.2	2.2	63
10	1.8	4.3	6.1	86.6	2538	769	–	–	–	–	–	569	1373	3.8	1.0	54	190	508	7.1	2.8	66
12	16.9	6.7	23.6	64.8	145109	700	379	4371	0.5	5.2	31	496	7846	4.7	9.4	56	185	309	6.6	3.0	44
14	31.0	3.6	34.6	44.5	26102	1114	400	3525	0.4	4.2	14	597	2811	3.7	3.4	11	346	1018	13.3	3.3	91
15	9.5	0.6	10.0	29.3	8340	1417	392	2696	0.5	4.0	32	542	1255	5.8	1.9	15	231	844	14.0	0.3	60
16	30.2	1.9	32.1	30.2	8325	–	–	–	–	–	–	548	6682	3.9	24.2	80	–	–	–	–	–
18	37.6	1.4	39.0	51.8	35419	387	374	27432	0.5	29.1	77	577	6610	3.6	7.0	19	324	232	7.2	0.9	60
19	23.9	17.1	41.0	54.7	9418	673	426	5109	0.4	13.0	54	597	2292	3.9	5.8	24	364	475	10.5	12.1	71
21	15.7	9.7	25.4	51.5	16829	930	393	13438	0.5	12.7	80	563	1364	3.8	1.3	8	222	745	10.8	7.8	80
22	18.9	2.3	21.2	44.5	32472	1078	444	4423	0.4	2.6	14	538	3589	4.3	2.1	11	391	576	10.4	1.2	53
23	24.2	2.1	26.3	53.6	37930	838	409	7061	0.4	4.5	19	548	4618	4.4	2.9	12	358	719	9.9	1.8	86
24	19.5	4.7	24.2	54.2	21288	167	422	4871	0.5	4.5	23	520	9538	3.9	8.8	45	359	167	12.2	4.7	100
25	15.2	0.1	15.3	65.9	9008	171	–	–	–	–	–	508	6492	3.8	11.0	72	317	171	17.0	0.1	100
27	34.4	3.4	37.8	57.7	50428	1188	613	6921	0.4	4.7	14	–	–	–	–	–	–	–	–	–	–
28	16.0	4.7	20.7	74.4	21740	736	493	5744	0.4	4.2	26	556	12635	3.4	9.3	58	309	320	5.3	2.0	43
29	20.0	2.6	22.6	72.6	23979	707	–	–	–	–	–	591	5829	2.8	4.9	24	173	316	5.8	1.2	45
30	9.3	2.7	12.0	70.9	15769	749	547	5056	0.4	3.0	32	562	7231	4.2	4.3	46	340	333	10.3	1.2	44
31	12.1	11.9	24.0	59.7	20480	4678	516	8055	0.5	3.5	39	588	7911	3.8	3.4	39	291	665	4.3	1.7	14
32	29.0	2.8	31.8	62.1	50815	816	552	10471	0.4	6.0	21	602	2545	2.4	1.5	5	318	356	6.3	1.2	44
33	23.2	4.0	27.2	52.7	36108	2243	578	1782	0.3	1.1	5	554	14363	2.9	9.2	40	308	1774	7.3	3.2	79
35	19.8	3.6	23.4	65.9	47255	1481	529	23416	0.6	9.8	50	979	1468	5.6	0.6	3	280	768	14.8	1.9	52
36	19.6	1.4	21.0	63.9	57580	–	540	4600	0.5	1.6	8	888	10974	11.5	3.7	19	–	–	–	–	–
37	4.2	7.6	11.8	72.8	5235	1596	381	546	0.4	0.4	10	540	1484	3.4	1.2	3	294	758	13.7	3.6	48
41	11.2	15.5	26.7	61.3	26537	4188	778	19640	0.6	8.3	74	889	2171	1.7	0.9	8	258	2740	8.0	10.1	65
42	4.1	4.4	8.5	54.9	13167	–	–	–	–	–	–	893	662	3.0	0.2	5	–	–	–	–	–
43	7.0	13.5	20.5	55.5	13405	3222	–	–	–	–	–	877	2077	2.0	1.1	15	340	1360	8.6	5.7	42
44	7.7	8.9	16.5	70.5	13229	2452	–	–	–	–	–	904	5119	2.3	2.6	39	404	1573	18.1	5.7	64
50	11.1	3.0	14.1	77.8	17272	747	–	–	–	–	–	889	4847	2.2	3.1	28	376	747	14.6	3.0	100
51	–	–	–	61.5	9605	1033	–	–	–	–	–	667	760	7.6	–	8	237	915	10.6	–	89
52	16.7	0.6	17.3	60.1	6520	897	532	4178	0.4	10.7	–	558	918	5.5	2.4	14	320	543	11.0	0.4	61
54	14.3	3.1	17.4	73.6	5573	978	–	–	–	–	–	621	4610	5.1	11.8	83	343	467	12.8	1.5	48
55	5.8	4.7	10.5	91.0	6111	–	–	–	–	–	–	655	4173	5.2	4.0	68	–	–	–	–	–

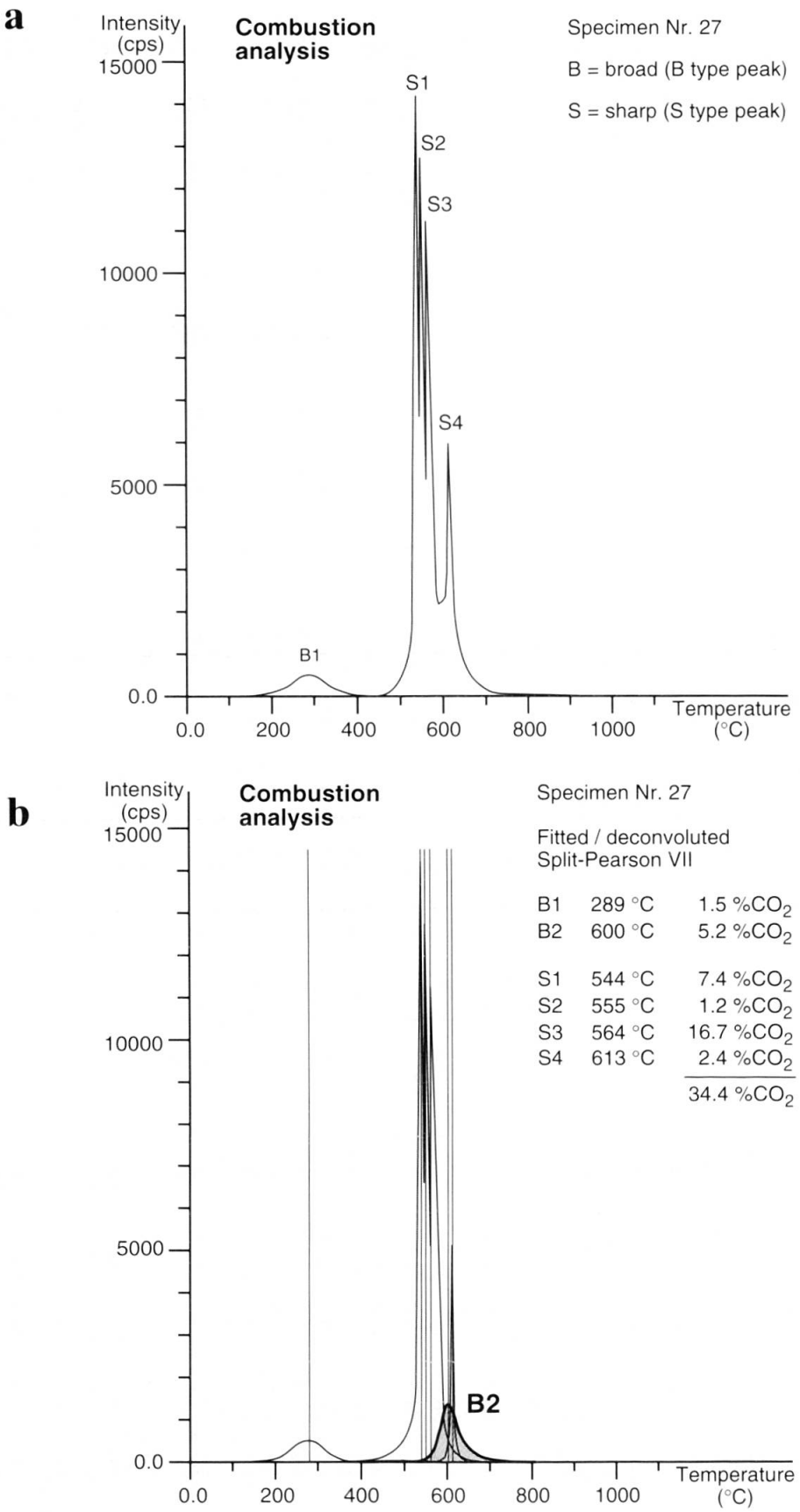

Fig. 3 Peak fitting applied to a typical reaction profile of specimen 27 from dynamic combustion analysis. A Split-Pearson VII fit of sharp type-S and broad type-B reactions is shown in Figure 3b. In Figure 3a a B2 reaction peak is assumed by the asymmetric shape of the S4 reaction peak. In Figure 3b a B2 peak is fitted by using the deconvolution technique. X-axis refers to reaction temperature (°C), Y-axis to intensity. Individual percentages of the involved CO_2 release are calculated from fitted peak areas. Peak/Apex temperatures and peak areas computed using peak fitting program by Bruker-AXS, Karlsruhe (Topas-P, V 1.0, DiffracPlus, 1998).

Table 2 Instrumental conditions.

X-ray diffraction [XRD]	
Apparatus	D-5000 (Bruker-AXS /Siemens, GFR)
Excitation	Cu-tube, 40 kV, 30 mA. Graphite monochromator, no primary filter. Variable divergence and antiscatter slits
Exposure	step size = 0.02 °2Θ, time = 10 sec, angular limits 25 to 29 °2Θ
Specimen	1 to 5 mg carbonaceous matter concentrate (including insoluble rutile, zircon, tourmaline, pyrite) on Makrofol (KG, Bayer GFR) foil 40 mm diameter (HANDSCHIN and STERN, 1989)
Combustion analysis [CA], dynamic operation mode	
Apparatus	RC-412 multiphase carbon determinator (Leco, USA)
Carrier gas	oxygen, 50 ml/min
Heating rate	70 °C/min, temperature range 60 to 1000 °C, parallel data registration
Sample	1 to 5 mg carbonaceous matter concentrate, porcelain vessels
Calibration	mixture of Merck calcite and gypsum (3.55 wt% C, 13.9 wt% H_2O)
Evaluation	data processing and conversion via Lotus 1-2-3 spread-sheet. Fitting/deconvolution by means of Split-Pearson VII functions, program Topas-P of Bruker-AXS, DiffracPlus, 1998
Thermal Analysis [DTA and TGA]	
Apparatus	STD 2960 (TA Instruments, USA)
Carrier gas	oxygen, 100 ml/min
Heating rate	20 °C/min, temperature range 60 to 1300 °C
Specimen	1 to 5 mg carbonaceous matter concentrate, Pt-cups, corundum inert reference

was restricted between 60 to 1300 °C. An advantage of DTA-TGA techniques is the high temperature attainable. Some small minor signals of the background pattern are probably related to the release of incorporated water and other exothermic reactions of the unsolved remaining heavy minerals; like the annealing of radiation damages in zircon. As shown in Fig. 2, zircon is a minor constituent of the unsolved mixture. By 1300 °C most reactions are terminated, whereas this is not the case at 1100 °C, the highest temperature reached in combustion analysis.

Differential thermal analysis has been applied to carbonaceous material in very few recent studies (WADA et al., 1994; KAHR et al., 1996). Simultaneous DTA-TG analysis (termed *thermal analysis* in what follows) determines the exo- or endothermic character of the reaction. By contrast to combustion analysis, it does not identify which signals are from water and carbon, respectively. In DTA-TG analysis under oxygen, OM is oxidizes in an exothermic reaction.

3.5. MACERAL ANALYSIS, VITRINITE AND BITUMINITE REFLECTANCE

124 samples (mostly sandy shales) along the profile were cut, mounted in epoxy resin and polished. First, by maceral analysis vitrinite was distinguished from macerals of the inertinite and liptinite maceral-group (cf. STACH et al., 1982) and from secondary macerals, like bituminite. The principal method used in the metamorphic profile of the Bündnerschiefer to determine metamorphic grade is the measurement of vitrinite reflectance (VR). Maximum ($\%R_{max}$) and minimum reflectance was measured. The metamorphic zones (high diagenesis, low and high anchizone, low and high epizone) between diagenesis and greenschist–blueschist facies are defined by illite cystallinity (IC) and correlated with VR. With the occurrence of optical graphite, maturity and illite studies are limited and metamorphic zones (facies) are defined by mineral assemblages.

Most samples yielded about 10 to 50 measuring points on average. More information about sampling, maceral determination and reflectance measuring are given by FERREIRO MÄHLMANN (1995). Measurements with less than 10 points, or a standard deviation of >10% and a relative variation-coefficient of > 5.0% were not used for correlation with IC. VR is a parameter sensitive to temperature in the range from 0.25 up to 8.0 $\%R_{max}$ (FERREIRO MÄHLMANN, 1995). This sensitivity diminishes with increasing rank from the zone of low diagenesis with ±0.05 $\%R_{max}$ to the epizone with ±1.0 $\%R_{max}$. In the studied area, VR ranges from 3.0 to 16.0 $\%R_{max}$, but with the determination of optical graphite between a VR of 8.0 and 16 $\%R_{max}$, most measurements are indicated in Table 1 as optical graphite.

Maximum and minimum reflectance were also measured for large and anisotropic bituminite fragments and vein fillings with a homogeneous extinction. In some samples bituminite gives a qualitative information about metamorphism in rocks without vitrinite phytoclasts. Using the correlation of bituminite- and vitrinite reflectance between 2.5 and 5.0 $\%R_{max}$ the bituminite reflect-

ance (BR) is used as a VR value (see FERREIRO MÄHLMANN, 2001). In shear zones and strongly foliated rocks, reflectance increases rapidly due to the formation of pre-graphite (pre-graphitization, initial formation stage of graphitoid spheroliths, cf. STACH et al., 1982) giving VR values of the semi-graphite stage (> 6.0 $\%R_{max}$).

4. Results

4.1. X-RAY DIFFRACTION

Most of the Bündnerschiefer samples studied were X-ray amorphous or produced diffuse reflections that could not be treated to obtain 2Θ or half-width values. In 12 cases only (of which 10 are displayed in Fig. 2), the (002) reflection was

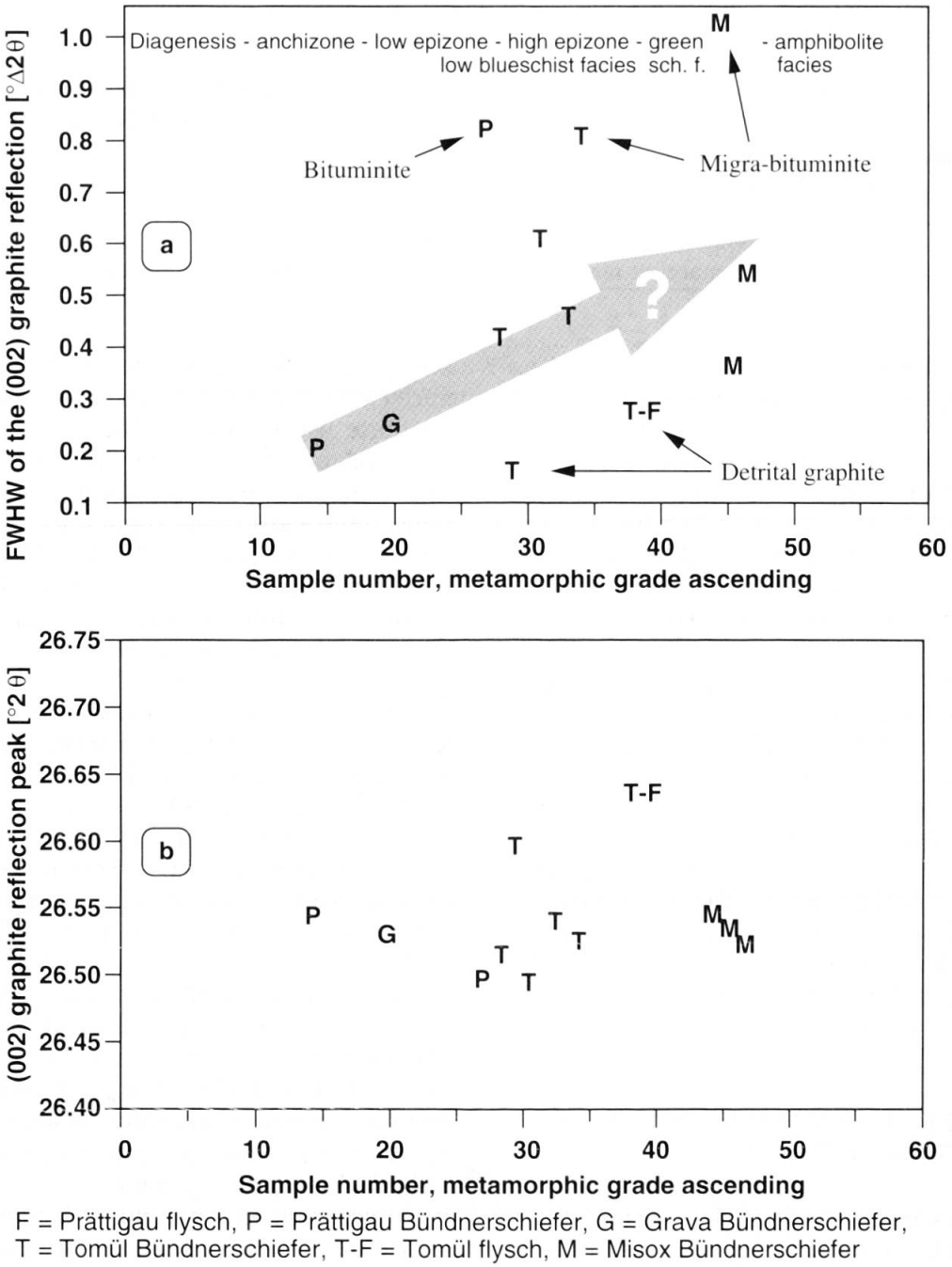

Fig. 4 X-ray diffraction of carbonaceous material concentrates. Shown are all samples with graphite peak areas > 500 net counts, with increasing metamorphic grade. (a) Full width at half maximum intensity [FWHM] values of the (002) reflection of graphite. For the correlation with metamorphic grade, values from samples where the main component is (1.) bituminite and migra-bituminite with a low structural order, and (2.) samples with derital graphite and consequently with a high structural order, are excluded. The trend shown can not be interpreted with the increase of metamorphic grade; the FWHW values should decrease. (b) 2Θ [Cu rad] values of the (002) reflection of graphite.

strong enough to be evaluated. The asymmetric shape of the (002) reflection suggests that the samples contain OM in variable stages of structural ordering (KRIBEK et al., 1994).

Previous studies found that carbonaceous materials in regionally metamorphosed rocks show continuous changes with increasing metamorphic grade, with a shift of the (002) graphite reflection towards higher diffraction angles (LANDIS, 1971; GREW, 1974; ITAYA, 1981; OKUYAMA-KUSUNOSE and ITAYA, 1987; PESQUERA and VALASCO, 1988; WADA et al., 1994). Well-ordered graphite appears at the onset of epidote-amphibolite or amphibolite facies conditions (LANDIS, 1971).

In nearly all Bündnerschiefer samples, detrital optical graphite populations occur. In the Prättigau and Tomül Flysch polymodal graphite reflectance histograms were obtained. Detrital graphite in lower grade metasedimentary rocks has been reported by many authors (DIESSEL et al., 1978; ITAYA, 1981). HRTEM studies by BUSECK and BO-JUN (1985) revealed fully-ordered graphite even in a chlorite-zone rock. In samples 1, 2, and 3 (Fig. 1) from the semi-anthracite to anthracite stage, correlating with an IC of high diagenesis, an anthracite to meta-anthracite and a semi-graphite peak were found by optical reflectance measurements. In the Tertiary units the detrital graphite population is generally dominant and can amount to 70 to 90 vol% of the OM (samples 1 to 4, 35 and 40).

The graphite crystallinity is defined as the full width at half maximum intensity (FWHM) of the (002) graphite reflection. The X-ray half width-values obtained [FWHM of areas >500] do not indicate a significant trend along the metamorphic profile (Fig. 4a). For the Prättigau area and around Chur, in Early Cretaceous Bündnerschiefer, maceral analysis show a relatively uniform OM composition of 50 to 70 vol% bituminite, 20 vol% inertinite, 5 to 10 vol% vitrinite (anthracite stage), and <10 vol% detrital vitrinite (meta-anthracite to semi-graphite stage) and detrital graphite populations (optical graphite). Due to the increase in metamorphic grade, in the Early Cretaceous formations in Chur, the vitrinite reflectance is close to the optical graphite jump (FERREIRO MÄHLMANN and PETSCHICK, 1997). Strong variations in the mean vitrinite reflectance values (5.7 $\%R_{max}$ in sample 10, around 8.0 $\%R_{max}$ in samples 11,13, 24 to 26) correspond to the transitional matter of DIESSEL et al. (1978). For the Prättigau area and around Chur (Prättigau-Flysch, Bündnerschiefer and Grava nappe) the graphite (002) reflection was strong enough to be evaluated only in samples 14, 19 and 26 (Fig. 4a). In contrast to previous studies (e.g. LANDIS, 1971; ITAYA, 1981; PESQUERA and VALASCO, 1988; WADA et al., 1994) no increase of graphite FWHM with metamorphic grade was observed, nor a shift of the (002) reflection towards higher angles (Fig. 4b).

With increasing metamorphic grade (samples 27 to 46) data show considerable scatter. No trend is obvious in the peak positions [°2Θ] of their (002) graphite reflection, nor in their FWHM (Fig. 4). These observations may indicate OM with different degrees of structural ordering and composition even at higher metamorphic grade (upper greenschist to lower amphibolite facies). In the area of Thusis and Splügen (Fig. 1), the inertinite component is very variable and ranges from 60 to 90 vol%. Close to nappe thrust planes, normal faults and shear zones pre-graphitization increases; but also oxidation due to weathering, ground water flow or metamorphic fluid circulation is frequently indicated by optical microscopy. All these factors can cause an enhancement of VR and different degrees of structural order.

On the other hand, at the front of the Middle Penninic nappes (Fig. 1a), migra-bituminite (post metamorphic migrated hydrocarbons) with a relative low reflectance (5.0 to 6.5 $\%R_{max}$) also occurs, in samples 35/36 and 37/38. Finally, in shear zones of the same area, a sub-microscopical graphite (micrinitic graphite) is typical, with tiny grains being dispersed in the sheet silicates. The organic origin is not clear. The broad variations in CM composition, of OM maturity from in-situ- and migra-bituminite, and in the degree of the OM pre-graphitization progress explains well the considerable scatter of FWHM and the peak positions of samples 27 to 46.

In the Tertiary flysch units (T-F, see Fig. 4) between Thusis and Splügen, small values of FWHM (0.28), and peak positions of 26.64 [°2Θ] prove the existence of ordered graphite (samples 35/36 to 40). In sample 40 detrital optical graphite is the dominant component of OM.

WINTSCH et al. (1981) found no correlation between variables measured by X-ray diffraction and metamorphic grade, and these authors suggested that variable fugacities of H_2 and CH_4 and/or variable permeabilities may be responsible for the non-uniform development of graphite crystallinity in the greenschist facies. Variable fugacities, oxidation by weathering, post-metamorphic infiltration of migra-bituminite, pre-graphitization by strain effects, micrinitic graphite and variable vitrinite-inertinite composition of OM together probably all contribute to the strong scatter of results for the Tomül-Misox Bündnerschiefer (Fig. 4).

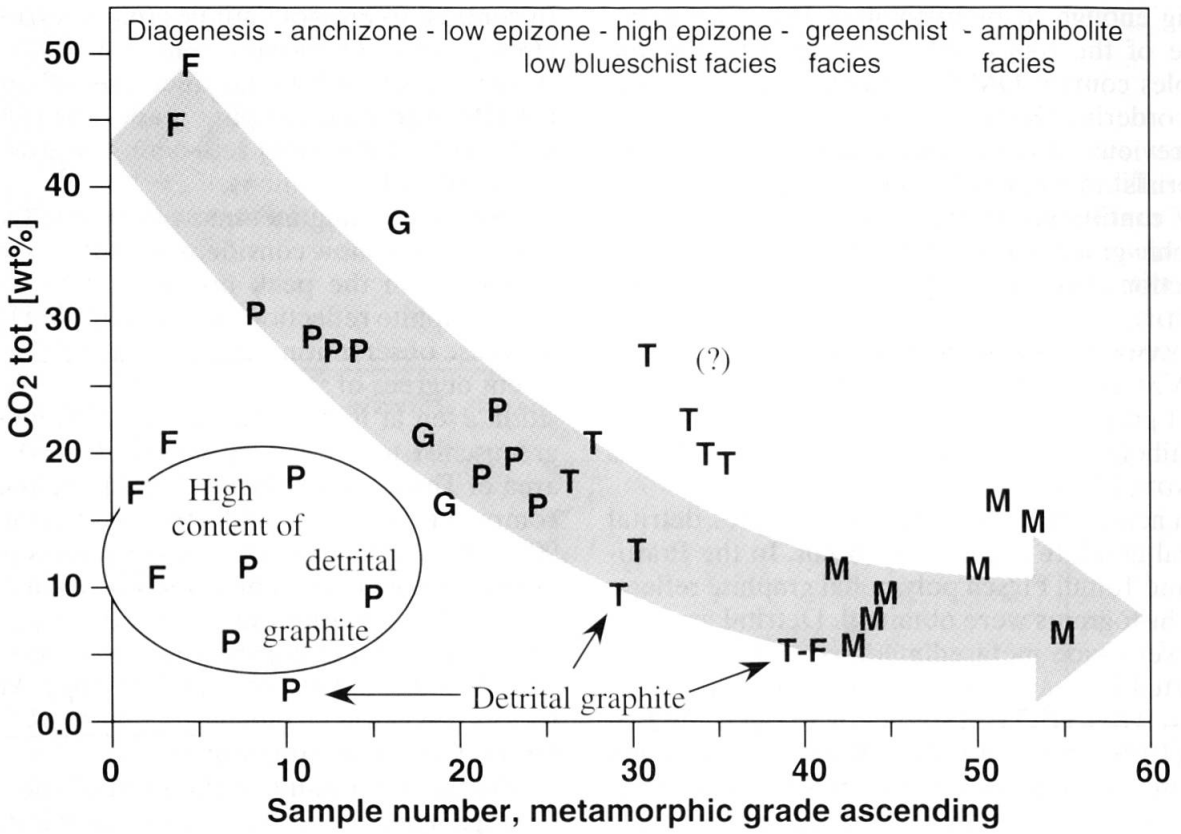

Fig. 5 Correlation of the CO_2 content of carbonaceous material concentrates with metamorphic grade. With increasing metamorphic grade the CO_2 content of OM according to combustion analysis decreases essentially. Heterogeneities in OM composition, detected by optical microscopy, are reflected in a sample group with a high amount of detrital graphite. This is specifically evident in samples 10, 28 and 40 were detrital optical graphite is the predominant constituent. For sample code see Fig. 4.

4.2. COMBUSTION ANALYSIS

The maximum total carbon content of OM in the Bündnerschiefer decreases with increasing metamorphic grade to one third of the high diagenetic value (Fig. 5). This trend parallels the release of H_2, H_2O, H_2S and CH_4 from the organic material during metamorphism (HUCK and KARWEIL, 1955; ITAYA, 1981; TEICHMÜLLER, 1987).

Samples show differences in the shape of the CO_2 peaks (signals) released during combustion analysis under oxygen. We distinguish two types of peaks: (a) sharp narrow CO_2 peaks (Fig. 6a) called type-S; (b) broad CO_2 peaks (Fig. 6b) denoted type-B. Each type of CO_2 signal is supposed to be related to a specific OM species, as elaborated below.

For metamorphic studies only the CO_2 peaks with the highest temperature of combustion are important since they correspond to the most thermally resistant and, hence, structurally more evolved forms of OM. Thus, amongst all strong type-S CO_2-peaks present in any sample, those released at the highest temperature were chosen for metamorphic studies.

Maceral analyses are available from a few samples only, hence the comparison between the peak types and the OM composition is preliminary. S-type signals may reflect different macerals of liptinite–bituminite origin. Type S-peaks are caused by a fast type of combustion reaction, probably due to the high H_2, H_2O, H_2S and CH_4 contents in liptinite and bituminite. In samples 3, 13 and 27 (Fig. 3a) different liptinite-bituminite populations are present correlating with several type-S peaks. Broader peaks indicate a slower oxidation process of the more thermally resistant vitrinite (O_2-rich macerals) or inertinite (C_2-rich macerals). Further work is needed to substantiate this result.

A disadvantage for the analysis of OM is the ubiquity of detrital optical graphite. A dominant detrital population with a high coalification rank can not reflect metamorphic grade. Graphite should represent the most thermally resistant organic material. Therefore, the signal at the highest temperature in some samples (e.g. sample 2) may reflect the detrital origin rather then the metamorphic grade. Nevertheless, for narrow CO_2 peaks the temperature values increase (Fig. 7a)

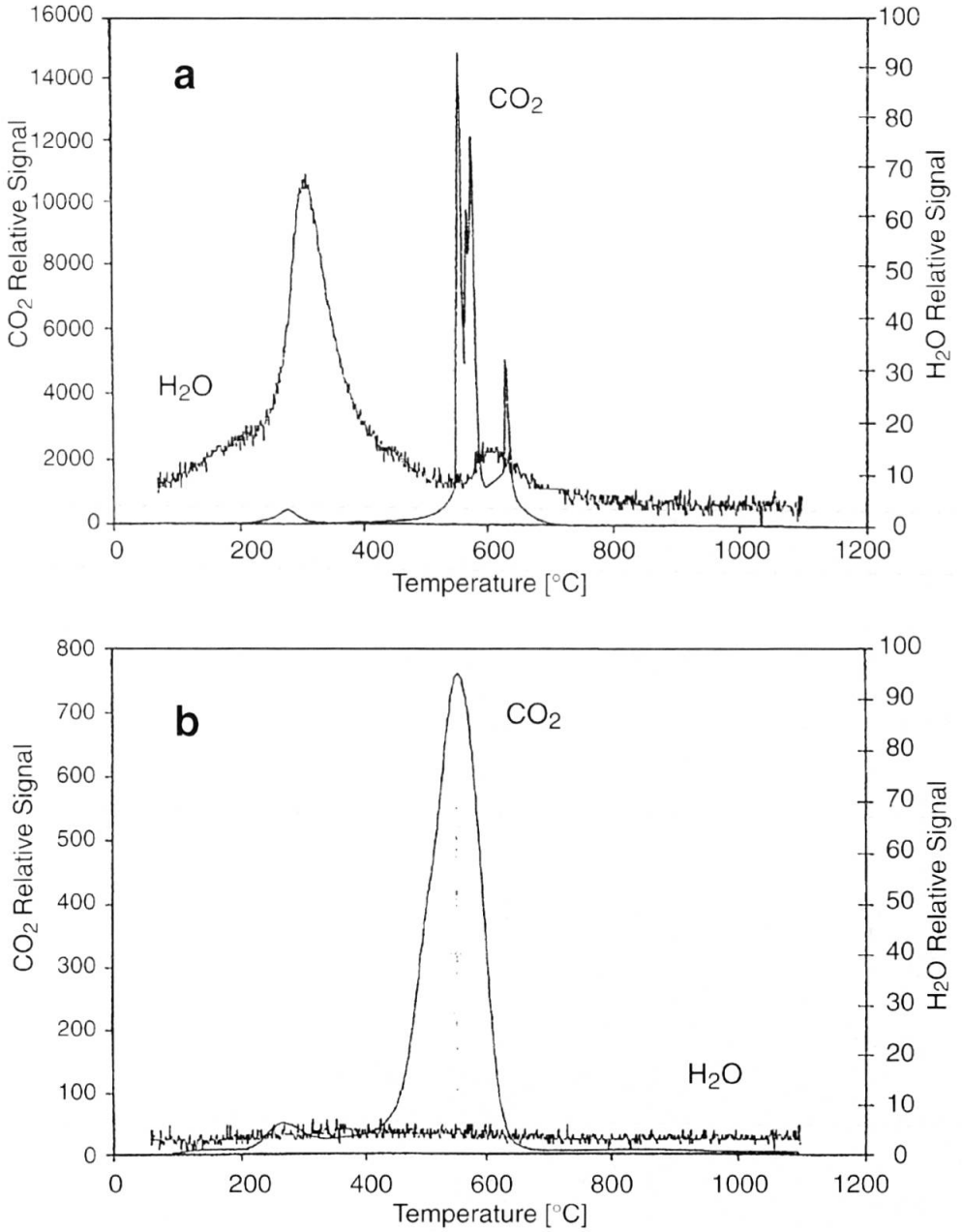

Fig. 6 Combustion analysis of two typical organic matter concentrates under oxygen. Signals due to CO_2 (intensity scale at left Y-axis) and H_2O (intensity scale at right Y-axis) are shown:
(a) Type-S: mainly strong, narrow and sharp CO_2 reaction peaks (sample 27, TP13)
(b) Type-B: only broad CO_2 reaction peaks (sample 16, TP06).

with increasing metamorphic grade. This supports the interpretation of gradual structural ordering of OM and of its increasing thermal resistivity with increasing metamorphic grade along the profile.

A slight increase of the reaction temperature is evident in the Prättigau units and the Grava nappe, but an important increase is visible at the hanging wall of the basal thrust fault of the Tomül nappe (Fig. 7a). In the Misox area, a S-type reaction was observed in two samples only, due to the disappearing H_2-rich macerals (liptinite and bituminite) in the epizone.

Broad B-type reaction peaks do not change along the metamorphic profile. In all stratigraphic units of the Prättigau-, Grava- and Tomül-Bündnerschiefer and Flysch units, an OM population of the semi-graphite stage is very frequently found. In contrast to S-type reactions, B-type reactions are a fingerprint of the detrital component. As the graphitization level of the detrital population in all samples is of the same semi-graphite stage, the combustion is probably limited to a restricted temperature range between 500 and 600 °C (Fig. 7b). In the greenschist facies the combustion temperature jumps suddenly to 850 to 900 °C; optical

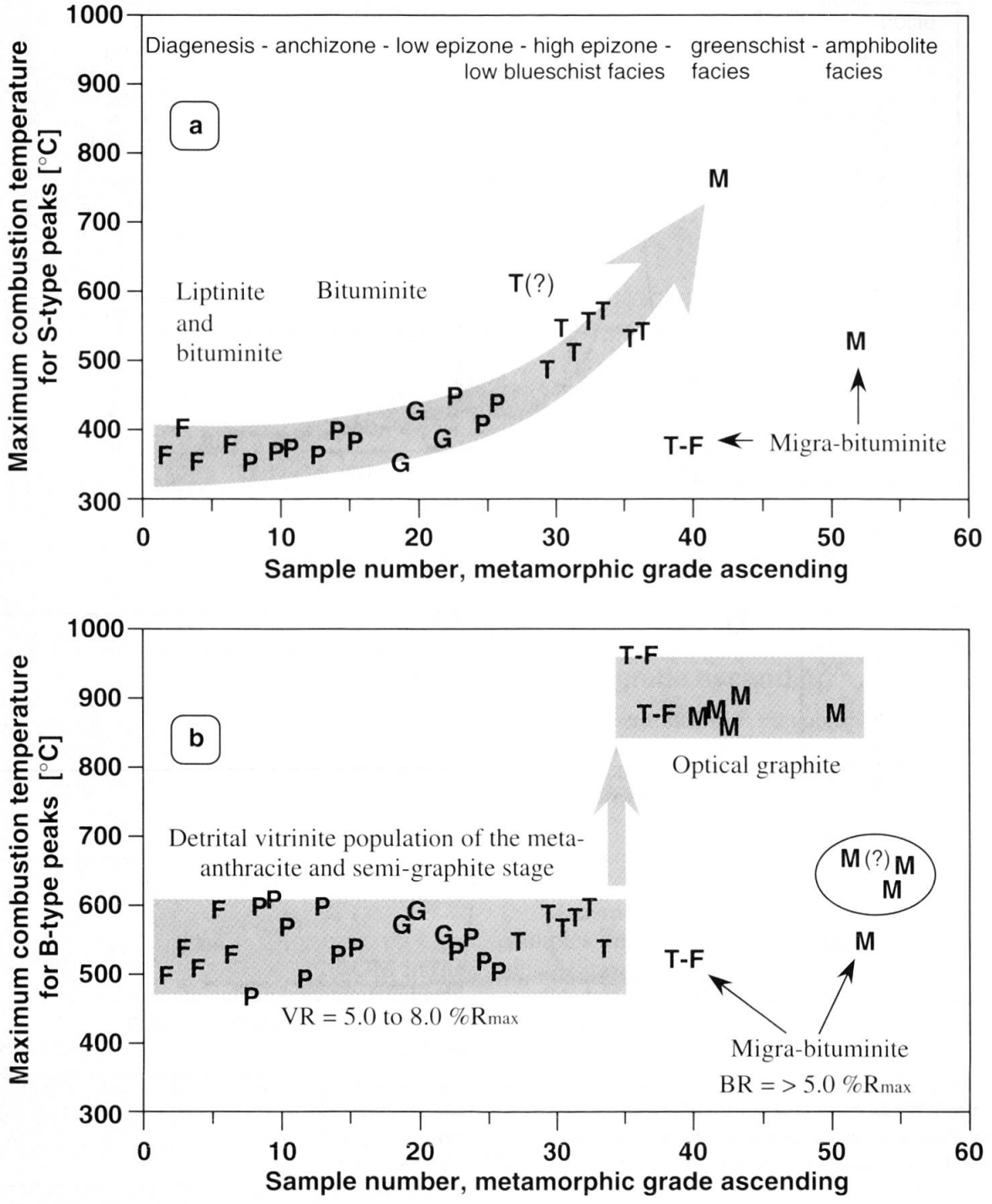

Fig. 7 Correlation of maximum reaction temperature of organic matter (OM) concentrates under oxygen with metamorphic grade. Reaction peaks with an area >500 net counts were plotted.
(a) Type-S: strong narrow sharp CO_2 reaction peaks. Those peaks are caused by H_2-rich macerals. At greenschist facies bituminite is consumed and volatilized at conditions corresponding to the transition from high epizone (low blueschist facies) to low greenschist facies. Samples 40, containig mostly optical graphite (Fig. 4), and 52 revealed under the microscope a migra-bituminite population. Both samples do not reflect metamorphic grade.
(b) Type-B: strong, broad CO_2 reaction peaks. Those peaks are caused by C_2- and O_2-rich macerals. As the graphitization level of the detrital population in samples 1 to 34 is of the same coalification stage, the combustion temperature is limited to a restricted temperature range. At the high epizone-low blueschist facies transition to greenschist facies the observed sudden increase of the combustion temperature is the result of reordering of the OM to a thermally more resistant optical graphite structure (samples 35 to 55).

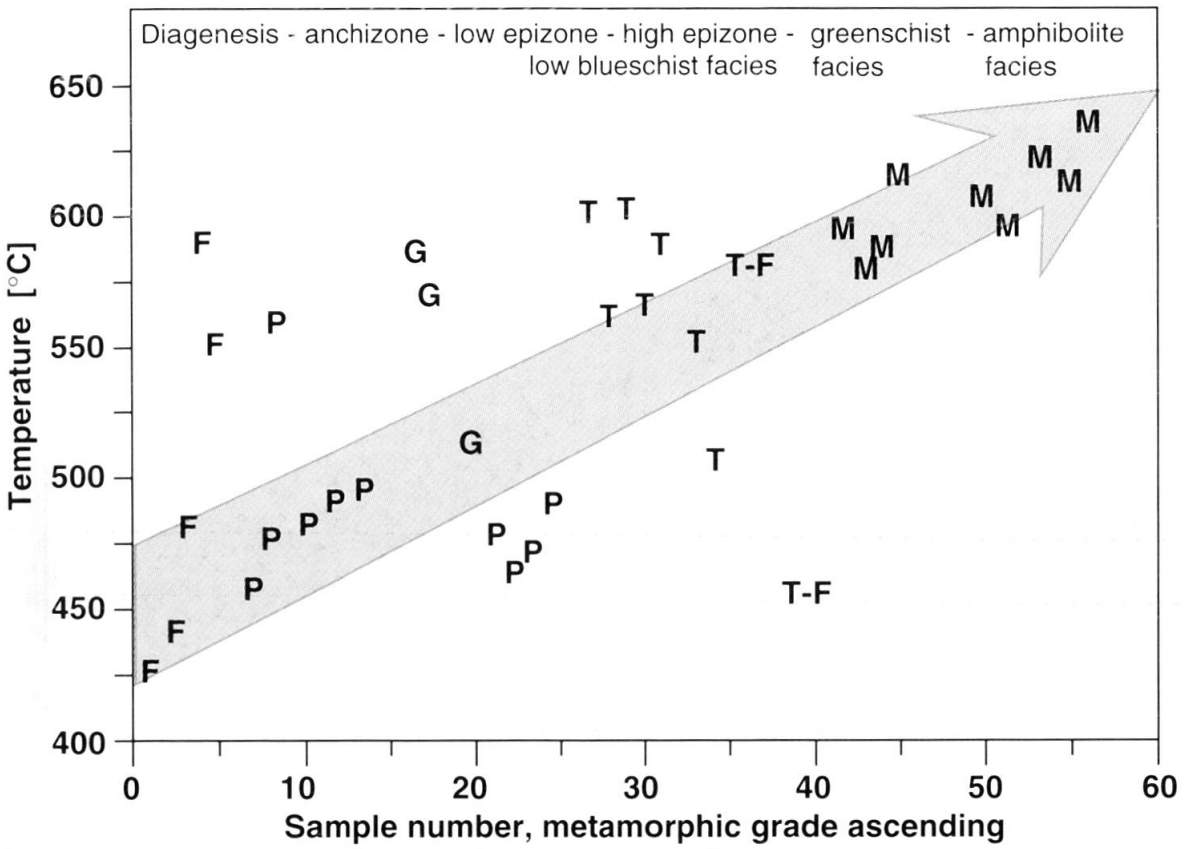

Fig. 8 Maximum temperatures of the DTA-TGA curves of organic matter (OM) concentrates, with oxygen as carrier gas. With increasing metamorphic grade, from left towards the right, maximum temperature increases. Code as in Fig. 7. Heterogeneities in OM composition causes a broad scatter at low metamorphic grade. Sample 40 containing migra-bituminite is strongly erratic.

graphite is then the only OM found. At amphibolite facies a sudden reversal down to 600 °C is observed; so far we cannot explain this result because few data are available at this high-temperature end of the metamorphic profile.

4.3. THERMAL ANALYSIS

In most cases thermal analysis indicates reactions of carbonaceous material with oxygen in the same temperature ranges as combustion analysis (Fig. 8). The slight shift in the reaction temperatures is attributed to differences in the heating rate. Furthermore, in thermal analysis the dehydroxylation reactions (loss of water) overlap with those of carbon dioxide release, and of oxidation of Fe^{2+} to Fe^{3+}.

As in combustion analysis, the DTA peaks at the highest temperature are of main interest for metamorphic studies. The increase in reaction temperature is diagnostic, reflecting the structural ordering in OM and its increasing thermal resistivity with increasing metamorphic grade.

Similar effects have been described by other researchers. WADA et al. (1994) compared graphitization trends for two metamorphic terrains, using X-ray diffraction and DTA data. They showed that the main exothermic peak temperature that corresponds to combustion of CM increases with increasing metamorphic grade.

KAHR et al. (1996) investigated bituminous claystone samples from different diagenetic and metamorphic grades, ranging up to lower amphibolite facies. The highest temperature of combustion of the organic substance in claystone samples was found to be a good indicator of metamorphic grade, and the maximum combustion temperature was shown to increase with increasing metamorphic grade. Our observations are in good agreement with these findings. Among the samples 1 to 25, some very low reaction temperatures are observed in the Prättigau Bündnerschiefer and in samples 35 and 37. The same specimens were characterized by type-S reactions in combustion analysis, and by higher bituminite contents. The high temperatures in samples 4 and 6 are probably due to their high contents of detrital optical graphite.

Total weight loss, as measured by thermal gravimetric analysis, decreases with increasing metamorphic grade (Fig. 9). This may be explained by the increasing carbon and decreasing water contents of OM with advancing graphitiza-

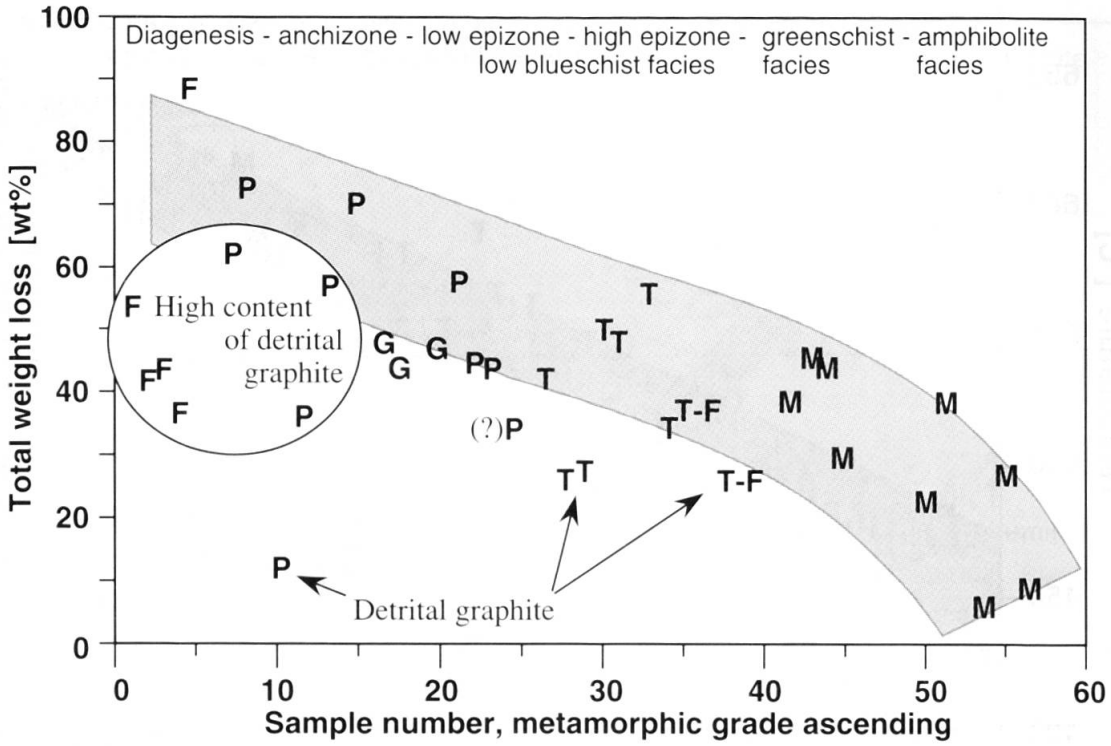

Fig. 9 Total weight loss of organic matter according to the thermal gravimetric analyses under oxygen. Samples listed with increasing metamorphic grade from left to right. Total weight loss results from release of volatile components and from oxidation. Heterogeneities in OM composition are reflected in the same sample group as in Fig. 5; in samples containing a high amount of detrital graphite. This is again specifically evident in samples 10, 28 and 40 were detrital optical graphite is the predominant constituent. Code as in Fig. 7.

tion, but also by the increasing modal abundance of insoluble accessory mineral phases (zircon, tourmaline, rutile, garnet) in the samples.

During thermal analysis of carbonaceous material from Bündnerschiefer, an interesting effect has been observed, denoted as DTA "loops": In case of a very fast reaction of OM under oxygen, and with high heating rate, these loops happen when the equipment overcompensates by strongly cooling down the furnace before continuing the heating process. Measurements at low heating rates (5 °C/ min and less) do not display loops but show well shaped exothermal DTA peaks instead.

However, DTA loops occur only in samples from a limited range of the metamorphic profile. In the high diagenesis and anchizone, and in the Tomül nappe, no correlation with the water contents of OM and with the sample weight is evident, but a correlation with the presence of the type-S CO_2-peaks from combustion analysis diagrams has been found. Loops and type-S peaks both disappear at higher anchizone of the metamorphic profile (Table 1). The type of OM producing narrow CO_2 peaks and DTA loops must be a thermally very reactive substance. Thus, as indicated in some samples by optical control, the correlation of the loops and the type-S peaks is very probably related to the occurrence of bituminite. At greenschist facies grade, bituminite is rare due to volatization, hence the peaks disappear. A few samples from low to medium metamorphic grade also show type-S signals. It is assumed that these local occurrences are caused by a secondary migra-bituminite, found at the northern front of the Middle Penninic nappes (Thusis, Splügen).

5. Discussion

5.1. BÜNDNERSCHIEFER METAMORPHIC PROFILE

Metamorphic grade increases continuously from samples 1 to 17, from high diagenesis (VR = 3.0 $\%R_{max}$, IC = 0.45 $\Delta°$ 2Θ, MA = kaolinite, glauconite, illite-smectite, corrensite, chlorite) to the epizone at Landquart (VR = 6.0 $\%R_{max}$, IC = 0.20 $\Delta°$ 2Θ, MA = clinozoisite, feldspars, muscovite/phengite, paragonite, chlorite–clinochlore, quartz, calcite) and at Chur (VR = 7.9 to 8.2.$\%R_{max}$, IC = 0.20 to 0.16 $\Delta°$ 2Θ, MA = clinozoisite, feldspars, muscovite/phengite, paragonite, chlorite–sudoitic clinochlore, quartz, calcite).

From Landquart to Chur vitrinite reflectance values increase from 7.0 ± 0.5 to 8.0 ± 0.5 $\%R_{max}$ and decrease again in the Grava nappe from Chur

to Thusis from 8.5 ± 1.0 to 7.0 ± 0.5 $\%R_{max}$. In this area vitrinite reflectance values of less than 7.0 ± 0.5 (min. 5.7 $\%R_{max}$) are too low, compared with the metamorphic grade defined by the mineral paragenesis of the low blueschist facies (sample 10, Table 1). It is known that high pressure conditions can retard VR (DALLA TORRE et al., 1996, 1997). A reflectance retardation is suggested for the core of both antiform structures in the Grava (Lunschania antiform) and Tomül nappe. At the north of Thusis the greenschist facies overprint did not pass higher temperature conditions of the older blueschist facies metamorphism. This is the reason why the blueschist facies metamorphic pattern and mineral assemblages were well preserved. Therefore, the metamorphic pattern in this area is presented on Fig. 1b with the signature of maximum metamorphic grade reached during low blueschist facies conditions. As an other consequence of those unchanged LT-HP conditions, at the south of Chur, a general pressure retardation of coalification and graphitization should be considered for the Grava- and Tomül Bündnerschiefer. Assuming a retardation of vitrinite reflectance, the specimens of the Grava nappe should be presented (in Figs. 5, 6, 8, and 9) with ascending grade between Prättigau and Tomül Bündnerschiefer samples. Trends in Figs. 5, 8, and 9 would then be more obvious yet, giving a linear function.

Between samples 12 and 24/25, 4 and 13, 34 and 35/36 metamorphic grade increases strongly. In these areas, connecting the three localities on an imaginary line, a disconformity in metamorphic grade is suggested to be related with a normal fault. A north–south shear zone is also evidenced by structural studies, but the fault could not be located in the field (WEH, 1998). Along that structure, the epizone in the northern part and the greenschist facies in the southern part, both contrast with blueschist facies conditions in the west (WEH et al., 1996). This zone will be denoted in what follows as the "Chur-Andeer zone" (see also FERREIRO MÄHLMANN and PETSCHICK, 1996). East of Thusis, P-T-conditions of 350 ± 50 °C and 4 ± 1 kbar (VR = 7.5 to 8.5 $\%R_{max}$, IC = 0.19 to 0.16 $\Delta°\ 2\Theta$, MA = clinozoisite, biotite, feldspars, muscovite, paragonite, chlorite–clinochlore, quartz, calcite) are badly constrained. Nevertheless, side by side, metamorphic grade is contrasting with conditions of 270 to 350 °C and 12 to 15 kbar (OBERHÄNSLI et al., 1995) at the west of the Chur-Andeer zone (VR = 7.0 to 9.5 $\%R_{max}$, IC = 0.20 to 0.14 $\Delta°\ 2\Theta$, MA = carpholite, phengite, paragonite, sudoitic chlorite–clinochlore, quartz, calcite).

Combining metamorphic studies and structural observations, it is very likely that the "tentatively traced carpholite isograde" by OBERHÄNSLI et al. (1995) has a tectonic reason. The blueschist facies metamorphic pattern is probably limited to the east by the north to south striking fault of the Chur-Andeer zone. Due to the progressive metamorphic hiatus a normal fault character is assumed, also, this structure may be linked with normal faulting at the "Turba mylonite zone" (NIEVERGELT et al., 1996). Deformation along the zone shows cross-cutting relations to the first foliation with the syn- to post-kinematic blueschist facies mineral assemblage (WEH, 1998) and cuts also folds of the second deformation. A synchronous formation age of the Chur-Andeer zone together with the Oligocene Turba mylonite zone seems to be possible.

Samples for carbonaceous studies were taken on the western part of the zone, except samples 35/36. Thus, between Chur and Thusis, metamorphic grade in the Bündnerschiefer profile increases steadily from north to south.

A vitrinite reflectance inversion occurs in the area of Andeer–Tiefencastel (FERREIRO MÄHLMANN, 1995); between the Arblatsch flysch (5.6 to 11.5 $\%R_{max}$) or the Tomül flysch (optical graphite) on one side and the Lenzerheide flysch (4.1 to 5.2 $\%R_{max}$) or the Tomül Bündnerschiefer (8 to 9.5 $\%R_{max}$) on the other. The metamorphic pattern at the Middle Penninic front is disturbed by post-greenschist facies metamorphic thrusting and normal faulting (FREY and FERREIRO MÄHLMANN, 1999). In the Suretta and Schams nappes no evidence for blueschist facies metamorphism is known, except for white micas with a high phengite component (BAUDIN and MARQUER, 1993). The tectono-metamorphic history is not well known in this area. Mineral paragenesis of the low greenschist facies and blueschist facies do not allow to reconstruct a metamorphic hiatus because slight differences in grade are not reflected by changes of the mineral assemblages and also the age of the different assemblages is not well known. Samples from the Bündnerschiefer at the Middle Penninic front (Piz Beverin) with chloritoid do not contain carpholite (RAHN and FREY, unpublished). In the Central Alps, the chloritoid-in isograde (beginning of the greenschist facies, BUCHER and FREY, 1994) was traced by FREY and WIELAND (1975), cross-cutting all nappe boundaries of the Helvetic and Penninic tectonic domain. But due to the young deformation of the VR-IC zones by folding and faulting in the North Penninic units and the discontinuity at the Helvetic-Penninic boundary (FERREIRO MÄHLMANN and PETSCHICK, 1996) also this isograde must be questioned. Therefore, in the "Map of Alpine Metamorphism of the Central Alps" the chloritoid occur-

rences in Graubünden were not linked by a mineral zone boundary south of the Helvetic domain (FREY and FERREIRO MÄHLMANN, 1999: Fig. 2).

From Splügen to Messoco metamorphism increases from low greenschist to low amphibolite facies. In this area VR and IC methods are no more sensitive to determine metamorphic grade (VR varies from 8.0 to 16 $\%R_{max}$ and IC from 0.26 to 0.13 $\Delta° 2\Theta$).

As evidenced from the front of the Middle Penninic units in the Tomül nappe, in-situ bituminite and migra-bituminite were formed during different stages of the metamorphic history. Secondary bituminite (migra-bituminite), of a lower reflectance (coalification) than primary bituminite (in-situ bituminite), may cause variations in the evolution pattern of the trends observed in Figs. 4, 5, 6 and 8. Note, that the late migration of hydrocarbon-rich fluids does not reflect the metamorphic conditions, but a step in the history of the thermal retrograde path. Data from these samples (samples 35 to 40) have to be interpreted with caution, also samples 44 and 52 from the Misox Bündnerschiefer.

5.2. METAMORPHISM OF ORGANIC MATTER IN THE BÜNDNERSCHIEFER PROFILE

Metamorphism of organic matter in Bündnerschiefer results in graphitization which is, however, not clearly reflected in the FWHM values from the (002) graphite reflection (Fig. 4a). Chemical changes (Fig. 5), an increase of OM combustion temperature (Figs. 7a and b), and a decreasing in the weight loss of OM in thermal analysis (Fig. 8) correlate with the graphitization process. The analytical methods applied demonstrate not only metamorphic changes, but also the heterogeneity of the carbonaceous material. Some types of heterogeneity are detected even within one locality (e.g. specimens 27 to 29), others are due to sampling in different structural units of Bündnerschiefer, where metamorphic processes may have proceeded in different ways.

Combustion analysis and optical data show that at least two types of OM can be clearly distinguished in Bündnerschiefer and Tertiary flysch units. One produces a sharp type-S CO_2 peak (Fig. 6a), the other produces broad type-B CO_2 peaks (Fig. 6b). The former are observed primarily in samples from the northern and middle part of the profile. Type-S peaks are absent in samples taken to the south of Thusis (Fig. 1, Table 1).

OKUYAMA-KUSUNOSE and ITAYA (1987) suggest that graphitization proceeds through two discontinuous changes: First, optically anisotropic domains develop within the coaly isotropic phytoclast. This is observed in vitrinite clasts at low diagenetic stages, not found in the Bündnerschiefer but in the Rhenodanubian flysch to the north of the studied metamorphic profile (FERREIRO MÄHLMANN, 1994). In a second step, transitional material is formed; and finally ordered graphite crystallizes at the expense of pre-existing OM. OKUYAMA-KUSUNOSE and ITAYA (1987) ascribe the apparently continuous variations in crystallographic parameters of the bulk OM to changes in the modal abundance of three types of OM: coaly, transitional materials, and graphite. The formation of transitional matter is evident in a large area between Chur, Thusis, and Tiefencastel. This is indicated by scatter in the vitrinite reflectance values between 5.7 to 10 $\%R_{max}$ at one locality (see also DIESSEL et al., 1978). At the south of Splügen, optical graphite is the dominant OM. Therefore, the subdivided classification into: (1) organic matter; (2) transitional matter; and (3) optical graphite from DIESSEL et al. (1978) can be also applied on the metamorphic Bündnerschiefer profile.

As shown for the Bündnerschiefer samples, both combustion types of peaks (S and B) are found in most samples from the high diagenesis to the high anchizone. We suppose that type-S corresponds to the coaly and transitional material of liptinite and bituminite macerals being consumed and volatilized at conditions corresponding to the transition from high anchizone to low greenschist facies in the area of Thusis. Type-B appears in those same samples where vitrinite, inertinite and detrital graphite are present. In the anchizone, two to three type-B peaks may reflect the presence of the three groups of OM vitrinite, inertinite and detrital graphite. Further work is needed to relate each signal to a specific maceral group. In the greenschist facies, better ordered graphite crystallizes at the expense of transitional material of vitrinite and probably also of liptinite and bituminite origin; this causes a single peak pattern in combustion analysis (Fig. 6b). At the moment, these results do not allow a direct comparison between optical data and combustion analysis.

In many samples, two to four sharp, narrow type-S CO_2 peaks are present (Fig. 6a). The highest number of these peaks is observed in only two parts of the profile, in the Prättigau Bündnerschiefer and the Tomül nappe Bündnerschiefer. The intensity of the sharp narrow peaks increases slightly in the Tomül nappe Bündnerschiefer. As shown by optical microscopy these observation can be related with the occurrence of bituminite. In both areas of the profile bituminite is an important component of OM. It is interesting to observe

that the main scatter of different parameters starts in the area of Thusis–Splügen, where a migra-bituminite population was found.

The sudden increase in peak temperature of type-S peaks in the Tomül nappe, reflecting a possible metamorphic discontinuity, has the same cause as the sudden higher vitrinite reflectance in the area at the south of Thusis at the Middle Penninic front. As badly constrained from vitrinite reflectance data, but based on the combustion reaction temperatures of this study, a metamorphic inversion is also supposed to occur between the Tomül nappe (high values, Table 1) and the Grava nappe (low values). The inversion is only of local importance, but shows that the metamorphic pattern at the Middle Penninic front is strongly disturbed by post-metamorphic deformation (FERREIRO MÄHLMANN, 1995).

From high diagenesis to epizone, including low greenschist and low blueschist facies, the combustion temperature of type-B reactions is probably mainly controlled by detrital vitrinite of the semi-graphite stage. At greenschist facies in the Tomül and Misox Bündnerschiefer, the sudden increase of reaction temperatures may be due to a structural change in OM. Optical microscopy in samples from the same area reveals a jump from meta-anthracite/semi-graphite values of around 8.0 $\%R_{max}$ to optical graphite (OG in Table 1), where reflectance values above 10 $\%R_{max}$ are found. This change is probably the result of the reordering of a two-dimensional aromatic plane structure to a three-dimensional crystal-like and thermally more resistant structure (see also TEICHMÜLLER, 1987; DEMENY, 1989).

Some of the sharp narrow type-S CO_2 peaks were followed by a DTA loop. This is notably the case for the northern part of the profile, north of Thusis (Table 1, Fig. 1). When comparing the coalification map at the boundary from Eastern to Central Alps (WEH et al., 1996) with the area where the loops are missing, it is evident that the missing loops coincide with a metamorphic high around Chur. Due to post-metamophic deformation of the Grava nappe the metamorphic high is located in the Lunschania antiform (WEH, 1998). Loops are missing also in the Misox Bündnerschiefer. In both sections of the metamorphic profile bituminite is decomposed and volatilized. These samples from the antiformal structure and the southern area contain OM dominantly in form of high coalified vitrinite (partly with retarded VR) which is less reactive under oxygen than the OM in form of bituminite which produces DTA loops. Due to slightly higher metamorphic grade and therefore higher graphitization in the antiform, loops were not develop.

Other heterogeneities observed may be explained by the coexistence of different kinds of OM in one locality or even inside one sample. BUSECK and BO-JUN (1985) described a sample with material that ranges from well-crystallized graphite to a poorly crystalline "circular" structure. They suggested that there may have been multiple sedimentary sources containing distinctive types of OM that contributed to these host rocks. DIESSEL et al. (1978), OKUYAMA-OKUNOSE and ITAYA (1987), and PESQUERA and VELASCO (1988) also reported the coexistence of OM with different texture and structure. LARGE et al. (1994) observed poorly crystalline CM in metasediments from chlorite to sillimanite grade, in contrast to most studies which observed well crystallized graphite already under upper greenschist conditions (TEICHMÜLLER, 1987). LARGE et al. (1994) explained the lack of graphitization as a consequence of a microporous structure of CM, combined with low oxygen fugacities in an internally buffered metamorphic fluid.

The main reason for scatter in the data is that the evolution through coaly, transitional materials, and to graphite is probably not a single process (OKUYAMA-KUSUNOSE and ITAYA, 1987) and, as shown in the present paper, is strongly dependent of the maceral groups and subgroups involved. It is also important to verify whether all components of the OM were coalified and formed cogenetically. The low reflecting migra-bituminite in the flysch of the Tomül nappe was probably condensed as solid exudatinite (asphalt exudates) from a liquid or gaseous phase in cracks and as cavity fillings after peak metamorphism (during cooling or a second metamorphic event). Bituminite and migra-bituminite can also be used to determine peak temperature conditions, but are useful indicators also of retrograde metamorphic conditions (FERREIRO MÄHLMANN et al., 2001; FERREIRO MÄHLMANN, 2001). For example, in some specimens of the Tomül flysch nappe and the Misox Bündnerschiefer, the presence of type-S peaks does not reflect the general increase in metamorphic grade from northeast to southwest.

6. Conclusions

Organic matter in Bündnerschiefer underwent graphitization during Alpine metamorphism. Carbon contents of carbonaceous material and water contents decrease along the metamorphic profile from N to S. Organic matter of primary inertinite or graphite-rich samples (detrital graphite) is water-poor, independent of the metamorphic grade. It seems that in Bündnerschiefer the water con-

tents mainly depend on the maceral group composition, they are not diagnostic of the metamorphic grade.

X-ray diffraction data were not effective in this study, although a slight increase of FWHM graphite (002) reflection values is observed along the profile. The combustion temperatures of organic matter increases essentially with increasing metamorphic grade, while the total weight loss decreases slightly. Combustion analysis was applied with very encouraging results; these correlate well with the known metamorphic pattern, and they also help to recognize tectonic structures and to clarify the tectono-metamorphic history.

Well-ordered graphite may still be associated with less-ordered organic material even in the lower amphibolite facies. Combustion analysis and differential thermal-thermal gravimetric analysis have proven to be useful in characterizing metamorphic organic matter and in detecting heterogeneities therein.

Work in progress will yield further data on the metamorphism of organic material in Bündnerschiefer, obtained through TEM, SEM, Raman and IR spectroscopy, carbon isotope studies, and a more systematic vitrinite reflectance and maceral study (FERREIRO MÄHLMANN et al., in preparation).

Acknowledgments

This study is part of the Ph.D. thesis of T. P. and was financially supported by the Swiss National Science Foundation, grant no. 20-56633.99. Vitrinite reflectance study and maceral analysis by R.F.M. were supported by the Swiss National Science Foundation, grant no. 21-50642.97. We thank Silvio Lauer (Basel) for the computation of Fig. 1 and Gerd Rantitsch (Leoben, A) for a constructive review of an earlier version. The manuscript has benefited greatly from thoughtful review, suggestions and revision of the English by Meinert Rahn (Freiburg, D). Discussions with Martin Engi, his detailed comments to a preview and careful final revision were of great help to us.

References

BUCHER, K. and FREY, M. (1994): Petrogenesis of Metamorphic Rocks. 6th edn. of Winkler's Textbook, Springer, Berlin, 318 pp.

BAUDIN, T. and MARQUER, D. (1993): Métamorphisme et déformation dans la nappe de Tambo (Alpes centrales suisses): évolution de la substitution phengitique au cours de la déformation alpine. Schweiz. Mineral. Petrogr. Mitt. 73, 285–299.

BUSECK, P.R. and BO-JUN, H. (1985): Conversion of carbonaceous material to graphite during metamorphism. Geochim. Cosmochim. Acta 49, 2003–2016.

CASTRO REIS, M.L.R.P. and CANTO MACHADO, M.J. (1992): An ultrasonic method for the separation of carbonaceous material from schists for the determination of graphitization degree by X-ray diffraction. Chem. Geol. 100, 191–199.

DALLA TORRE, M., DE CAPITANI, C., FREY, M., UNDERWOOD, M.B., MULLIS, J. and COX, R. (1996): Very low-grade metamorphism of shales from the Diablo Range, Franciscan Complex, California, USA: new constraints on the exhumation path. Geol. Soc. Am. Bull. 108, 578–601.

DALLA TORRE, M., FERREIRO MÄHLMANN, R. and ERNST, W.G., (1997): Pressure dependance of the maturation rate of organic matter. Geochim. Cosmochim. Acta 61/14, 2921–2928.

DEMENY, A. (1989): Structural ordering of carbonaceous matter in penninic terranes. Acta Mineralogica-Petrographica, Szeged 30, 103–113.

DIESSEL, C.F.K., BROTHERS, R.N. and BLACK, P.M. (1978): Coalification and graphitization in high-pressure schists in New Caledonia. Contrib. Mineral. Petrol. 68, 63–78.

DIETRICH, V.J. (1976): Plattentektonik in den Ostalpen: Eine Arbeitshypothese. Geotekt. Forsch. 50, 1–84.

FERREIRO MÄHLMANN, R. (1994): Zur Bestimmung von Diagenesehöhe und beginnender Metamorphose – Temperaturgeschichte und Tektogenese des Austroalpins und Süpenninikums in Vorarlberg und Mittelbünden. University of Frankfurt, Frankfurter geowiss. Arb., Serie C, 14, 498 pp.

FERREIRO MÄHLMANN, R. (1995): Das Diagenese-Metamorphose-Muster von Vitrinitreflexion und Illit-"Kristallinität" in Mittelbünden und im Oberhalbstein. Teil 1. Bezüge zur Stockwerktektonik. Schweiz. Mineral. Petrogr. Mitt. 75, 85–122.

FERREIRO MÄHLMANN, R. (1996): Das Diagenese-Metamorphose-Muster von Vitrinitreflexion und Illit-"Kristallinität" in Mittelbünden und im Oberhalbstein. Teil 2: Korrelation kohlenpetrographischer und mineralogischer Parameter. Schweiz. Mineral. Petrogr. Mitt. 76, 23–46.

FERREIRO MÄHLMANN, R. (2001): Correlation of very low grade data to calibrate a thermal maturity model in a nappe tectonic setting, a case study from the Alps. Tectonophysics 334, 1–33.

FERREIRO MÄHLMANN, R. and PETSCHICK, R. (1996): The coalification map of the Alps between the rivers Inn, Isar and Rhein (Austria and Switzerland): thermo-tectonic relations. MinPet. 96, Schwaz, Mitt. österreich. mineral. Ges. 141, 85–86.

FERREIRO MÄHLMANN, R. and PETSCHICK, R. (1997): The coalification map of the Alps between the rivers Inn, Isar and Rhein (Austria and Switzerland): thermo-tectonic relations: Terra Abstracts, Terra nova, 9, Abstract Supplement, No. 1, 576.

FERREIRO MÄHLMANN, R., BELMAR, M. and CIULAVU, M. (2001): Bituminite reflectance in very low grade metamorphic studies. Terra Abstracts, EUG 11, Diagenesis and Low-Grade Metamorphism, J. Conference Abstracts 6/1, 230.

FERREIRO MÄHLMANN, R., PETROVA, T., PIRONON, J., STERN, W.B., GHANBAJA, J., DUBESSY, J. and FREY, M. (in press): Transmission electron microscopy study of carbonaceous material in a metamorphic profile from diagenesis to amphibolite facies (Bündnerschiefer, Eastern Switzerland). Schweiz. Mineral. Petrogr. Mitt. 82/2, submitted to the special volume "Diagenesis and Low-Grade Metamorphism".

FREY, M. and WIELAND, B. (1975): Chloritoid in autochthon-parautochthonen Sedimenten des Aarmassives. Schweiz. Mineral. Petrogr. Mitt. 55/3, 407–418.

FREY, M. and FERREIRO MÄHLMANN, R. (1999) Alpine metamorphism of the Central Alps. Schweiz. Mineral. Petrogr. Mitt. 79, 135–154.

FREY, M., DESMONS, J. and NEUBAUER, F. (eds, 1999): The new metamorphic map of the Alps: Schweiz. Mineral. Petrogr. Mitt. 79(1).

GREW, E.S. (1974): Carbonaceous material in some metamorphic rocks of New England and other areas. J. Geol. 82, 50–73.

HANDSCHIN, R. and STERN, W.B. (1989): Preparation and Analysis of Microsamples for X-Ray Diffraction and -Fluorescence. Siemens Analytical Application Note 319.

HOEFS, J. and FREY, M. (1976): The isotopic composition of carbonaceous matter in a metamorphic profile from the Swiss Alps. Geochim. Cosmochim. Acta 40, 945–951.

HUCK, G. and KARWEIL, J. (1955): Physikalisch-chemische Probleme der Inkohlung: Brennstoff-Chemie 36, 1–11.

ITAYA, T. (1981) Carbonaceous material in pelitic schists of the Sanbagawa metamorphic belt in central Shikoku, Japan. Lithos 14, 215–224.

JÄGER, E. and STRECKEISEN, A. (1958): Nachweis von Graphit in graphitführenden Schiefern des Simplon-Gebietes (Wallis, Schweiz). Schweiz. Mineral. Petrogr. Mitt. 38/2, 375–386.

KAHR, G., FREY, M. and MADSEN, F.T. (1996): Thermoanalytical dehydroxylation of clays and combustion of organic compounds in a prograde metamorphic Liassic black shale formation, Central Swiss Alps. Schweiz. Mineral. Petrogr. Mitt. 76, 165–173.

KRIBEK, B., HRABAL, J., LANDAIS, P. and HLADIKOVA, J. (1994): The association of poorly ordered graphite, coke and bitumens in greenschist facies rocks of the Ponikla Group, Lugicum, Czech Republic: the result of graphitization of various types of carbonaceous matter. J. Metamorphic Geol. 12, 493–503.

LANDIS, C.A. (1971): Graphitization of dispersed carbonaceous material in metamorphic rocks. Contrib. Mineral. Petrol. 30, 34–45.

LARGE, D.J., CHRISTY, A.G. and FALLICK, A.E. (1994): Poorly crystalline carbonaceous matter in high grade metasediments: implications for graphitisation and metamorphic fluid compositions. Contrib. Mineral. Petrol. 116, 108–116.

MORIKIYO, T. (1984): Carbon isotopic study on coexisting calcite and graphite in the Ryoke metamorphic rocks, northern Kiso district, central Japan. Contrib. Mineral. Petrol. 87, 251–259.

NÄNNY, B. (1948): Zur Geologie der Prättigauschiefer zwischen Rhätikon und Plessur: PhD thesis, ETH Zürich, N.F. 276, 206 pp.

NIEVERGELT, P., LINIGER, M., FROITZHEIM, N. and FERREIRO MÄHLMANN, R. (1996): Early to Mid Tertiary crustal extension in the Central Alps: The Turba Mylonite Zone (Eastern Switzerland). Tectonics 15/2, 329–340.

OBERHÄNSLI, R., GOFFÉ, B. and BOUSQUET, R. (1995): Record of a HP-LT metamorphic evolution in the Valais zone: Geodynamic implications. In: LOMBARDO, B. (ed.): Studies on metamorphic rocks and minerals of the western Alps. Boll. Mus. Reg. Sci. nat. Torino 13/2, 221–240.

OKUYAMA-KUSUNOSE, Y. and ITAYA, T. (1987): Metamorphism of carbonaceous material in the Tono contact aureole, Kitakami mountains, Japan. J. Metamorphic Geol. 5, 121–139.

PASTERIS, J.D. and WOPENKA, B. (1991): Raman spectra of graphite as indicators of degree of metamorphism. Can. Mineral. 29, 1–9.

PESQUERA, A. and VELASCO, F. (1988): Metamorphism of the Paleozoic Cinco Villas massif (Basque Pyrenees): illite crystallinity and graphitization degree. Mineral. Mag. 52, 615–625.

RAGOTT, J.P. (1977): Contribution à l'étude de l'evolution des substances carbonées dans les formations géologiques. Unpublished PhD thesis, Univ. Toulouse, 150 pp.

SPÖTL, C., HOUSEKNECHT, D.W. and JAQUES, R.C. (1998): Kerogen maturation and incipient graphitization of hydrocarbon source rocks in the Arkoma Basin, Oklahoma and Arkansas: a combined petrographic and Raman spectrometric study. Org. Geochem. 28, 9/10, 535–542.

STEINMANN, M. (1994): Ein Beckenmodell für das Nordpenninikum der Ostschweiz. Jb. Geol. B.-A. 137/4, 675–721.

TEICHMÜLLER, M. (1987): Organic material and very low-grade metamorphism. In: FREY, M. (ed.): Low Temperature Metamorphism. Blacky, Glasgow and London, 114–161.

TEICHMÜLLER, M. and TEICHMÜLLER, R. (1954): Die stoffliche und strukturelle Metamorphose der Kohle. Geol. Rdsch. 42, 265–296.

TEUTSCH, R. (1982): Alpine Metamorphose der Misoxer-Zone (Bündnerschiefer, Metabsasite, granitische Gneise). Unpublished PhD thesis, Bern.

THOMPSON, P.H. (1976): Isograd patterns and pressure-temperature distributions during regional metamorphism. Contrib. Mineral. Petrol. 57, 277–295.

THUM, I. and NABHOLZ, W. (1972): Zur Sedimentologie und Metamorphose der penninischen Flysch- und Schieferabfolgen im Gebiet Prättigau-Lenzerheide-Oberhalbstein. Beitr. Geol. Karte Schweiz, N.F. 144, 55 pp.

TRÜMPY, R.(1980): Geology of Switzerland a Guide-Book. Part A: An Outline of the Geology of Switzerland, Wepf & Co., Basel, New York, 102 pp.

WADA, H., TOMITA, T., MATSUURA, K., IUCHI, K., ITO, M. and MORIKIYO, T. (1994): Graphitization of carbonaceous matter during metamorphism with references to carbonate and pelitic rocks of contact and regional metamorphism, Japan. Contrib. Mineral. Petrol. 118, 217–228.

WEH, M. (1998): Tektonische Entwicklung der penninischen Sediment-Decken in Graubünden (Prättigau bis Oberhalbstein). Unpublished PhD thesis, Basel University, 296 pp.

WEH, M., FERREIRO MÄHLMANN, R. and FROITZHEIM, N. (1996): Strukturelle und metamorphe Diskontinuitäten im Penninikum am Westrand der Ostalpen. In: AMANN, G., HANDLER, R., KURZ, W., STEYRER, H. P. (eds): VI. Symposium Tektonik – Strukturgeologie – Kristallingeologie. Facultas Univ.-Verl., Salzburg, Extended abstracts, 479–482.

WINTSCH, R.P., O'CONNELL, A.F., RANSOM, B.L. and WIECHMANN, M.J. (1981): Evidence for the influence of CH_4 on the crystallinity of disseminated carbon in greenschist facies rocks, Rhode Island, USA. Contrib. Mineral. Petrol. 77, 207–213.

WOPENKA, B. and PASTERIS, J.D. (1993): Structural characterization of kerogens to granulite-facies graphite: applicability of Raman microprobe spectroscopy. Am. Mineral. 78, 533–557.

YUI, T.F., HUANG, E. and XU, J. (1996): Raman spectrum of carbonaceous material: a possible metamorphic grade indicator for low-grade metamorphic rocks. J. Metamorphic Geol. 14, 115–124.

ZIEGLER, W. (1956): Geologische Studien in den Flyschgebieten des Oberhalbsteins (Graubünden). Eclogae geol. Helv. 49, 1–78.

Manuscript received November 15, 1999; revision accepted February 8, 2002.